PLANE WAVE DIFFRACTION BY A LARGE SEMICIRCULAR CYLINDRICAL BOSS

A Thesis

Presented to the Faculty

of the Department of Electrical Engineering

University of Houston

In partial Fulfillment

of the Requirements for the Degree

Master of Science

---

by

Richard Allen Meador

May 1969

ACKNOWLEDGMENT

The author wishes to thank Dr. G. Tyras for the opportunity to study this topic, for his generous consideration, and for his support and guidance. I wish to thank Dr. H. S. Hayre for his suggestions and support throughout my graduate program. Also, thanks to Dr. D. R. Williams for serving on the thesis committee.

The assistance and consideration given me by Texaco's Bellaire Laboratory is appreciated.

To my wife, Beverly, goes special thanks for preparing the manuscript.

This work was in part supported under contract NAS-9-6760.

PLANE WAVE DIFFRACTION BY A LARGE SEMICIRCULAR CYLINDRICAL BOSS

An Abstract of A Thesis
Presented to the Faculty
of the Department of Electrical Engineering
University of Houston

In partial Fulfillment
of the Requirements for the Degree
Master of Science

---

by
Richard Allen Meador
May 1969

ABSTRACT

The diffraction of a plane wave by a large semicircular cylindrical boss on a plane of infinite extent has been studied by application of the Watson Transformation. Three cases are considered: plane ground wave incidence, vertically polarized oblique plane wave incidence, and horizontally polarized oblique plane wave incidence. The transformed solutions give physical meaning to the diffraction process by isolating each contribution. The results show the diffraction to be composed of three primary terms: "creeping waves", waves reflected from the boss, and waves reflected from the ground plane. Numerical calculations are made comparing the classical "harmonic series" with the transformed solution. These calculations show good agreement with the classical results. Some plots of the normalized magnetic or electric field are given for the three cases. An approximate method for studying the imperfectly conducting boss and ground plane is suggested.

TABLE OF CONTENTS

LIST OF FIGURES

Figure Page

CHAPTER 1

INTRODUCTION

The problem of diffraction by a semicircular cylindrical boss on a flat, perfectly conducting ground plane of infinite extent has been solved by many authors. These solutions have been used to study the influence of a ridge or island on VLF communication (e.g., Wait and Murphy; 1957, 1958). They have also been used as the elements in rough surface scattering studies (Twersky; 1952, 1957). In general, these "harmonic series" solutions are useful for electrically small bosses, i.e., long-wavelength low frequency limits. For electrically large bosses, they are of little value because of their very slow convergence.

The "harmonic series" may be transformed into a more rapidly convergent series by application of the Watson Transformation (Franz, 1957, 1960; Tyras 1969; et. al.). This transformation, applied to cylinders, yields the "residue series" representation. This solution is highly convergent for large cylindrical radii. Also, the "residue series" solution is of particular value because it gives insight into the physical nature of the diffraction process. This solution has been shown to be important in the space shadowed by the cylinder.

For the illuminated region, a closed form approximation to the solution can be obtained. This solution is known as the "geometrical optics" approximation. Its accuracy depends primarily on the radial size of the cylinder. This results from the higher order terms of the approximation varying inversely with the electrical radius of the cylinder (Franz, 1957). For large cylinders, it is highly accurate.

The "residue series" solution and "geometrical optics" approximation have not been applied to a semicircular boss on an infinite ground plane. Therefore, the primary purpose of this thesis is the transformation of the slowly convergent "harmonic series" into the more convergent form for large bosses.

Three cases are considered. The first studies plane ground wave diffraction. The second and third cases study obliquely incident vertically and horizontally polarized plane wave diffraction. For these cases, each diffracted wave is isolated and discussed. Numerical calculations are then made comparing the results of 1) the transformed series with those of the "harmonic series" for plane ground wave diffraction, 2) oblique incidence vertically polarized plane wave diffraction with plane ground wave diffraction, and 3) horizontally polarized plane wave diffraction with vertically polarized plane wave diffraction.

An approximate method for extending the solution obtained from perfectly conducting boundaries to handle the imperfect case is suggested.

CHAPTER 2

FIELD EVALUATION FOR PLANE GROUND WAVE INCIDENCE

2.1 General Problem Development

The problem of the diffraction by a large semi-cylindrical boss, shown in Figure 1, is approached and solved in the classical manner.

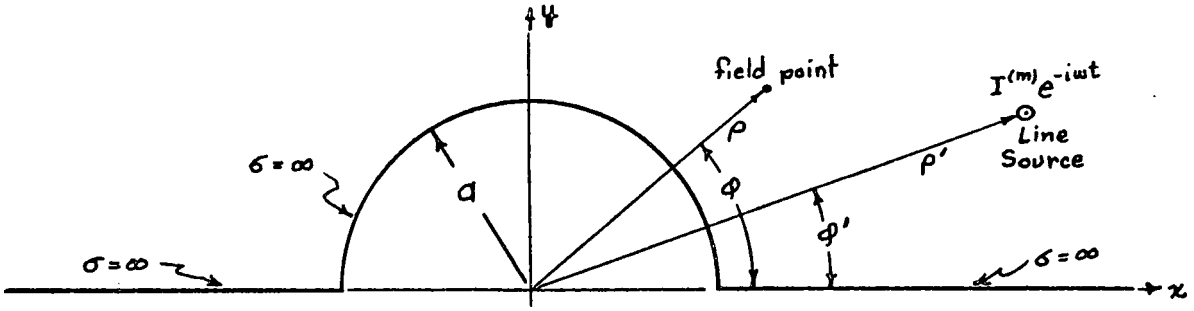

Figure 1. Semicircular cylindrical boss on an infinite ground plane.

In terms of the Hertzian magnetic vector, the wave equation and associated electromagnetic fields are given by

$$(\nabla^2 + k_o^2)\,\overline{\Pi}^{(m)} = \frac{-i}{\omega\mu_o}\,\overline{J}^{(m)}, \tag{1}$$

$$\overline{E} = i\omega\mu_o\,\nabla \times \overline{\Pi}^{(m)}, \tag{2}$$

$$\overline{H} = k_o^2\,\overline{\Pi}^{(m)} + \nabla(\nabla\cdot\overline{\Pi}^{(m)}). \tag{3}$$

To generate the axially invariant vertically polarized wave, the magnetic current density, $\overline{J}^{(m)}$, is expressed as a line current by

$$\overline{J}^{(m)} = I^{(m)}\,\frac{\delta(\rho-\rho')\,\delta(\phi-\phi')}{\rho}\,\overline{a}_z$$

where ρ and ϕ represent the field coordinates and ρ' and ϕ' the source coordinates. A ground wave can be obtained by setting ϕ' equal to zero. A plane wave is obtained by allowing ρ' to approach infinity.

Since the current density is axial, only the z-component of the Hertzian magnetic vector will be nonzero. Thus (1) may be written as a scalar equation,

$$\left[\frac{1}{\rho}\frac{\partial}{\partial\rho}\left(\rho\frac{\partial}{\partial\rho}\right) + \frac{1}{\rho^2}\frac{\partial^2}{\partial\phi^2} + k_o^2\right]\Pi_z^{(m)} = \frac{-i\,I^{(m)}}{\omega\mu_o}\frac{\delta(\rho-\rho')\,\delta(\phi-\phi')}{\rho} \tag{4}$$

Also, since the plane and boss are perfectly conducting, the boundary conditions are given by

$$\begin{aligned} \frac{\partial\,\Pi_z^{(m)}}{\partial\,\rho} &= 0 \qquad \text{at} \qquad \rho = a \\ \frac{\partial\,\Pi_z^{(m)}}{\partial\,\phi} &= 0 \qquad \text{at} \qquad \phi = 0,\pi \end{aligned} \tag{5}$$

The solution to (4) is well known and is obtained by separation of variables techniques (Jones, 1964). The solution is given as

$$\Pi_{z\,\rho<\rho'}^{(m)} = \frac{-I^{(m)}}{2\omega\mu_o}\sum_{m=0}^{\infty}\epsilon_m\cos m\phi\cos m\phi'\,H_m^{(1)}(k_o\rho')\left\{J_m(k_o\rho) - \frac{J_m'(k_o a)}{H_m^{(1)\prime}(k_o a)}H_m^{(1)}(k_o\rho)\right\} \tag{6}$$

where the primes denote derivatives with respect to the Bessel function argument. Setting ϕ' equal to zero and allowing ρ' to approach infinity, (6) becomes

$$\Pi_{z\,\rho<\rho'}^{(m)} = \frac{-I^{(m)}}{2\omega\mu_o}\sqrt{\frac{2}{\pi k_o\rho'}}\,e^{i(k_o\rho'-\pi/4)}\sum_{m=0}^{\infty}\epsilon_m\cos m\phi(-i)^m\left\{J_m(k_o\rho) - \frac{J_m'(k_o a)}{H_m^{(1)\prime}(k_o a)}H_m^{(1)}(k_o\rho)\right\} \tag{7}$$

Substituting (7) into (3), the magnetic field intensity is

obtained as

$$H_z = H_o \sum_{m=0}^{\infty} \epsilon_m (-i)^m \cos m\varphi \left\{ J_m(k_o\rho) - \frac{J_m'(k_o a)}{H_m^{(1)\prime}(k_o a)} H_m^{(1)}(k_o\rho) \right\} \tag{8}$$

where $$H_o = \frac{-I^{(m)} \omega \epsilon_o}{\sqrt{2\pi k_o \rho'}} e^{i(k_o\rho' - \pi/4)}$$

Noting a well-known addition theorem in Bessel functions (Watson, 1944), the incident wave is given by

$$H_z^{inc.} = H_o \sum_{m=0}^{\infty} \epsilon_m (-i)^m \cos m\varphi \; J_m(k_o\rho) = H_o e^{-ik_o\rho\cos\varphi}$$

Thus, the magnetic field intensity for ground wave incidence may be written as

$$H_z = H_o \left\{ e^{-ik_o\rho\cos\varphi} - \sum_{m=0}^{\infty} \epsilon_m (-i)^m \frac{J_m'(k_o a)}{H_m^{(1)\prime}(k_o a)} H_m^{(1)}(k_o\rho) \right\} \tag{9}$$

The solution given by (8) or (9) can be used to calculate the field amplitudes for any size cylindrical boss. However, the series in (9) is very slowly convergent when $k_o a > 1$. Hence many terms are required for accuracy. The field given by (9) has previously been evaluated for bosses as large as three wavelengths (Wait & Murphy, 1958; Webster, 1966). The convergence of the series in (8) can be improved by application of the Watson Transformation.

2.2 Transformation of the Classical Harmonic Series.

Shadow Region. The classical "harmonic series" solution for ground wave incidence is given by (8). However, it is not in a form which can be readily transformed. Examining

the series and using some well-known trigonometric and Bessel function identities, (8) may be recast as

$$H_z = H_0 \sum_{m=-\infty}^{\infty} (-i)^m e^{im\varphi} \left\{ J_m(k_0\rho) - \frac{J_m'(k_0a)}{H_m^{(1)\prime}(k_0a)} H_m^{(1)}(k_0\rho) \right\} . \tag{10}$$

The series given by (10) is exactly the same solution as obtained for a cylinder with an incident plane wave at zero degrees (Jones, 1964). The solution is, however, subject to a slightly different interpretation. That is, for the boss, $0 \leq \varphi \leq \pi$; while for the cylinder, $0 \leq \varphi < 2\pi$.

The "harmonic series" given by (10) has been transformed previously (Franz, 1957; Tyras, 1969). The highlights of that transformation are given below.

Consider the integral

$$H_z = \frac{i}{2} \oint_C \frac{e^{i\nu(\varphi - \pi)}}{\sin \nu\pi} B_\nu^{(m)} \, d\nu \quad , \tag{11}$$

where

$$B_\nu^{(m)} = H_0 \frac{e^{-i\nu\pi/2}}{H_\nu^{(1)\prime}(k_0a)} \left\{ H_\nu^{(1)\prime}(k_0a) \, J_\nu(k_0\rho) - J_\nu'(k_0a) \, H_\nu^{(1)}(k_0\rho) \right\}$$

$$B_\nu^{(m)} = \frac{H_0}{2} \frac{e^{-i\nu\pi/2}}{H_\nu^{(1)\prime}(k_0a)} \left\{ H_\nu^{(1)\prime}(k_0a) \, H_\nu^{(2)}(k_0\rho) - H_\nu^{(2)\prime}(k_0a) \, H_\nu^{(1)}(k_0\rho) \right\}$$

and the contour C is taken, as shown in Figure 2, to include the poles due to the zeroes of $\sin \nu\pi$.

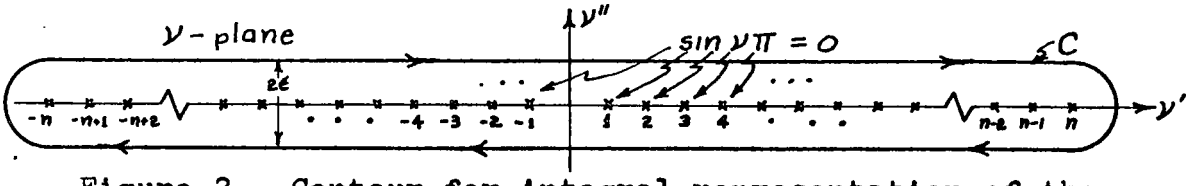

Figure 2. Contour for integral representation of the "harmonic series" solution.

By the theory of residues, (11) may be shown to equal the "harmonic series", (10), provided that B_ν does not have singularities on the real axis. In addition, since B_ν is an even function, i.e., $B_\nu = B_{-\nu}$, (11) becomes

$$H_z = i\int_{-\infty+i\epsilon}^{\infty+i\epsilon} \frac{\cos\nu(\varphi-\pi)}{\sin\nu\pi} B_\nu^{(m)}\, d\nu \quad , \tag{12}$$

where ϵ raises the integration path slightly above the real axis.

The integral given by (12) is then evaluated by closing the contour in the upper half ν-plane. The poles due to $\sin\nu\pi$ have now been excluded. However, the poles due to the zeroes of $H_\nu^{(1)\prime}(k_0a)$ are captured in the process (Tyras, 1969). Thus, the contour is taken as shown in Figure 3.

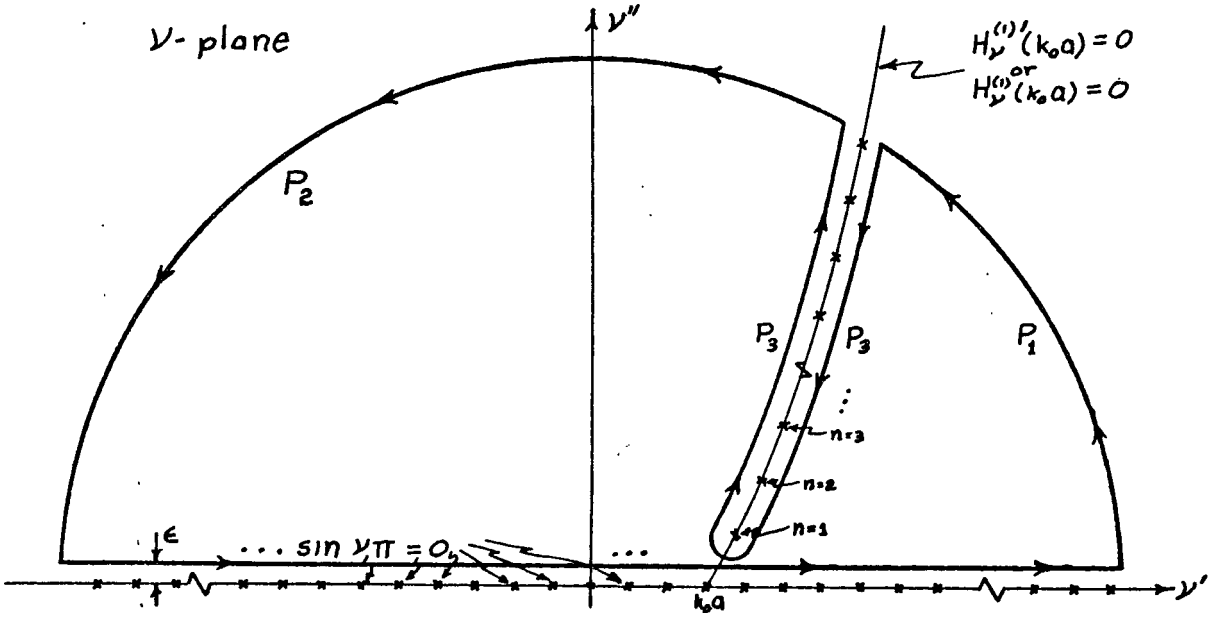

Figure 3. Deformed contour for integral representation of the "harmonic series" solution.

Applying the theory of residues to (12) and the contour in Figure 3,

$$i\int_{-\infty+i\epsilon}^{\infty+i\epsilon} \frac{\cos\,\nu(\phi-\pi)}{\sin\,\nu\pi}\, B_\nu^{(m)}\, d\nu \;-\; 2\pi \sum_{n=1}^{\infty} \text{residues @ } \nu=\nu_n' \;=0,$$

provided the contribution of the contour paths P_1 and P_2 vanish at infinity. By application of the infinite ν-plane, Debye asymptotic forms to $B_\nu^{(m)}$ (Franz; 1957, 1960) and allowing $|\nu|\longrightarrow\infty$, the contributions of P_1 and P_2 will vanish for field angles greater than $\pi/2$.

Thus,

$$H_z = H_o\pi\sum_{n=1}^{\infty} \frac{H_{\nu_n'}^{(2)\prime}(k_o a)}{\frac{\partial}{\partial\nu} H_\nu^{(1)\prime}(k_o a)\Big|_{\nu=\nu_n'}} \frac{\cos\,\nu_n'(\phi-\pi)}{\sin\,\nu_n'\pi}\, e^{-i\nu_n'\pi/2}\, H_{\nu_n'}^{(1)}(k_o\rho) \qquad (13)$$

where ν_n' is the n^{th} zero of $H_\nu^{(1)\prime}(k_o a)$ as obtained from the Airy function representation of the Hankel function. In addition, $H_{\nu_n'}^{(2)\prime}(k_o a)$ and $\frac{\partial}{\partial\nu}H_\nu^{(1)}(k_o a)\Big|_{\nu=\nu_n'}$ can be expressed by their Airy function representations (Tyras, 1969). So that (13) becomes

$$H_z = \frac{H_o}{2}\, e^{-i\pi/6}\left(\frac{k_o a}{2}\right)^{1/3}\sum_{n=1}^{\infty} \frac{\cos\,\nu_n'(\phi-\pi)\; e^{-i\nu_n'\pi/2}}{a_n'[Ai(a_n')]^2\,\sin\,\nu_n'\pi}\, H_{\nu_n'}^{(1)}(k_o\rho)\;, \qquad (14)$$

where

$$\nu_n' = k_o a \;- a_n'\left(\frac{k_o a}{2}\right)^{1/3} e^{-i\pi/3}$$

and a_n' are the zeroes of the first derivative of the Airy function with respect to its argument.

The solution given by (14) is known as the residue series representation. Since this series converges for field

angles greater than 90 degrees, it is applicable only in the shadow region of the cylindrical boss. It is, however, of no value for field calculations in the illuminated region.

Illuminated Region. A representation which allows field evaluation in the illuminated region may be obtained by suitable transformation of the original integral representation, (12). Noting the relationship

$$\cos \nu(\varphi - \pi) = e^{i\nu\pi} \cos \nu\varphi - i e^{i\nu\varphi} \sin \nu\pi$$

(12) becomes

$$H_z = \int_{-\infty+i\epsilon}^{\infty+i\epsilon} \left\{ B_\nu^{(m)} e^{i\nu\varphi} + i \frac{e^{i\nu\pi} \cos \nu\varphi}{\sin \nu\pi} B_\nu^{(m)} \right\} d\nu \qquad (15)$$

The second term in the braces in (15) is of the same form as (12) and is evaluated in the same manner. Thus, (15) becomes

$$H_z = \frac{H_o}{2} e^{-i\pi/6} \left(\frac{k_o a}{2}\right)^{1/3} \sum_{n=1}^{\infty} \frac{\cos \nu_n' \varphi \, e^{-i\nu_n'\pi/2}}{a_n' [Ai(a_n')]^2 \sin \nu_n' \pi} H_{\nu_n'}^{(1)}(k_o\rho) + \int_{-\infty+i\epsilon}^{\infty+i\epsilon} B_\nu^{(m)} e^{i\nu\varphi} d\nu \qquad (16)$$

Substituting $B_\nu^{(m)}$ into the remaining integral, one obtains

$$\int_{-\infty+i\epsilon}^{\infty+i\epsilon} B_\nu^{(m)} e^{i\nu\varphi} d\nu = \int_{-\infty+i\epsilon}^{\infty+i\epsilon} (H_o/2) H_\nu^{(2)}(k_o\rho) e^{i\nu(\varphi-\pi/2)} d\nu - \frac{H_o}{2} \int_{-\infty+i\epsilon}^{\infty+i\epsilon} H_\nu^{(1)}(k_o\rho) \frac{H_\nu^{(2)\prime}(k_o a)}{H_\nu^{(1)\prime}(k_o a)} e^{i\nu(\varphi-\pi/2)} d\nu \qquad (17)$$

It is noted that the first integral in (17) is zero, since $H_\nu^{(2)}(k_o\rho)$ has no poles in the upper half ν-plane. The second integral is equal to the contribution of contour P_3 and is evaluated by the method of stationary phase to be to the first order

$$\int_{-\infty+i\epsilon}^{\infty+i\epsilon} B_\nu^{(m)} e^{i\nu\varphi}\, d\nu = H_o \Big\{ e^{-ik_o\rho\cos\varphi} + \sqrt{\frac{a\cos\beta}{2\sqrt{\rho^2 - a^2\sin^2\beta} - a\cos\beta}}\, e^{ik_o\left(\sqrt{\rho^2 - a^2\sin^2\beta} - a\cos\beta\right)} \Big\}, \tag{18}$$

where β is as shown in Figure 4. This solution is known as the geometrical optics approximation for the solution in the illuminated region.

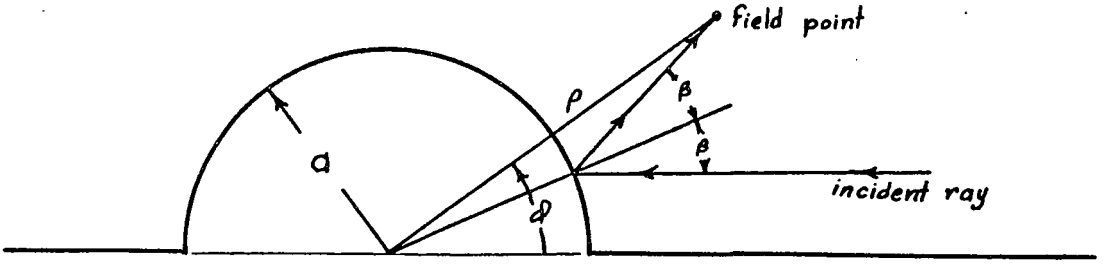

Figure 4. The geometrical definition of β for the illuminated zone.

Collecting all the terms,

$$H_z = H_o \Big\{ e^{-ik_o\rho\cos\varphi} + \sqrt{\frac{a\cos\beta}{2\sqrt{\rho^2 - a^2\sin^2\beta} - a\cos\beta}}\, e^{ik_o\left(\sqrt{\rho^2 - a^2\sin^2\beta} - a\cos\beta\right)} + \frac{1}{2} e^{-i\pi/6} \left(\frac{k_o a}{2}\right)^{1/3} \sum_{n=1}^{\infty} \frac{\cos\nu_n'\varphi\; e^{-i\nu_n'\pi/2}}{a_n'[Ai(a_n')]^2 \sin\nu_n'\pi} H_{\nu_n'}^{(1)}(k_o\rho) \Big\}. \tag{19}$$

To the first order, (19) is the new representation of the magnetic field intensity in the illuminated zone.

2.3 Physical Interpretation of the Solution.

Shadow Zone. The solutions obtained are of particular value because physical insight into the diffraction by the cylindrical boss may be obtained.

Returning to (14), the magnetic field intensity in the shadow region, and noting the asymptotic form of $H^{(1)}_{\nu_n'}(k_o\rho)$ for $k_o\rho > \nu_n' \sim k_o a$ (Tyras, 1969) and the trigonometric identity

$$\frac{\cos \nu_n'(\phi - \pi)\; e^{-i\nu_n'\pi/2}}{\sin \nu_n'\pi} = -i\,\frac{e^{i\nu_n'(\phi - \pi/2)} + e^{i\nu_n'(3\pi/2 - \phi)}}{1 - e^{i\nu_n' 2\pi}}$$

(14) becomes

$$H_z = -\frac{H_o e^{i\pi/12}}{\sqrt{2\pi k_o \sqrt{\rho^2 - a^2}}}\left(\frac{k_o a}{2}\right)^{1/3} \sum_{n=1}^{\infty} D_n^{(m)} \left\{ e^{i[k_o\sqrt{\rho^2 - a^2} + \nu_n'(\phi - \pi/2 - \arccos a/\rho)]} \right. \tag{20}$$
$$\left. + \; e^{i[k_o\sqrt{\rho^2 - a^2} + \nu_n'(3\pi/2 - \phi - \arccos a/\rho)]} \right\},$$

where

$$D_n^{(m)} = \frac{1}{(1 - e^{i\nu_n' 2\pi})\, a_n' [Ai(a_n')]^2}$$

Examining (20), it is noted that the series is rapidly convergent for $\phi > \pi/2 + \arccos a/\rho$, since ν_n' has a rapidly increasing positive imaginary part. In addition, since $\nu_1' \sim k_o a$, the phase factors of (20) may be expressed respectively as

$$\Phi_1 = k_o[\sqrt{\rho^2 - a^2} + a(\phi - \pi/2 - \arccos a/\rho)]$$

and

$$\Phi_2 = k_o[\sqrt{\rho^2 - a^2} + a(3\pi/2 - \phi - \arccos a/\rho)]$$

Plots of the lines of constant phase, $\Phi_1 =$ constant and $\Phi_2 =$ constant, are given in Figure 5 and Figure 6. From these plots, it is clear that the first terms of the series in (20) represent the direct diffracted waves, while the second terms represent the diffracted waves which are reflected from the shadow region ground plane.

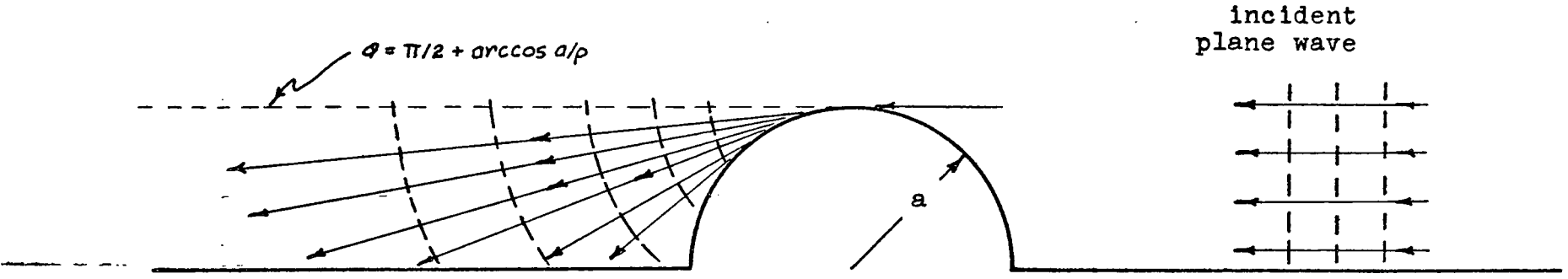

Figure 5. Lines of constant phase and propagation vectors for the term $e^{i[k_0\sqrt{\rho^2-a^2} + \nu_n'(\phi-\pi/2-\arccos a/\rho)]}$, --------- constant phase lines, ←——— propagation vectors.

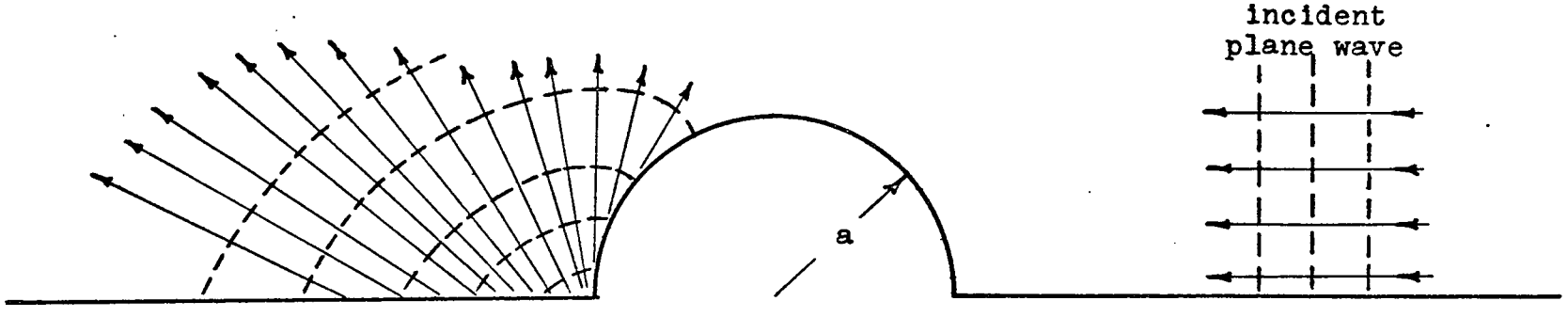

Figure 6. Lines of constant phase and propagation vectors for the term $e^{i[k_0\sqrt{\rho^2-a^2} + \nu_n'(3\pi/2-\phi-\arccos a/\rho)]}$, ---------constant phase lines, ←——— propagation vectors.

More specifically, the rays which arrive tangent to the cylindrical boss, $\phi = \pi/2$ in this case, travel along the cylindrical surface through an arc distance of $\phi - \pi/2 - \arccos a/\rho$ and $3\pi/2 - \phi - \arccos a/\rho$ radians. The surface currents induced by the tangential magnetic field then radiate the energy into the shadow region through a distance of $\sqrt{\rho^2 - a^2}$. The ray which travels the arc of $\phi - \pi/2 - \arccos a/\rho$ radiates directly to the field point; while the ray which travels through $3\pi/2 - \phi - \arccos a/\rho$ radians radiates toward the image of the field point in the ground plane, and is reflected by the ground plane to the field point, as shown in Figure 7.

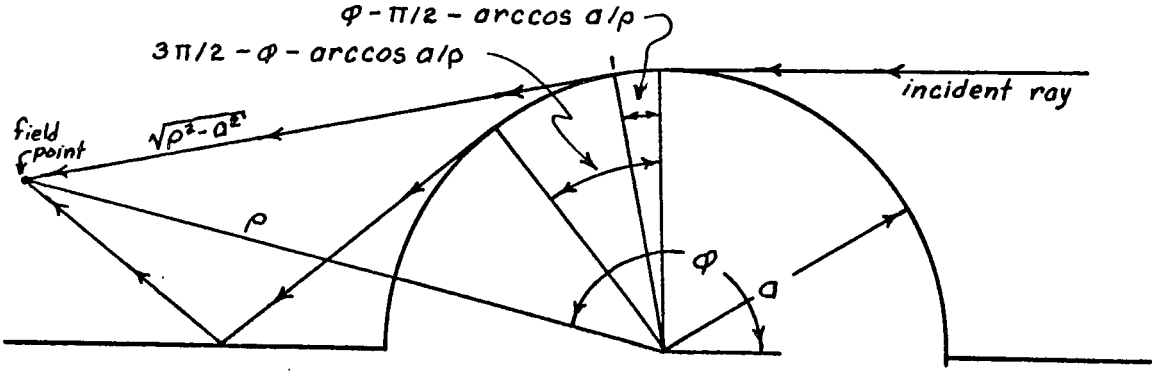

Figure 7. Shadow region creeping waves and geometry in ray form.

The imaginary part of ν_n' is proportional to the attenuation factor of the wave traveling on the cylindrical surface. In addition, since the real part of ν_n' is actually a little larger than $k_o a$, the velocity of the wave propagating along the cylinder's surface is lower than the free space velocity. Hence, this wave has been designated as a

"creeping wave".

Illuminated zone. Investigating the solution for the magnetic field intensity in the illuminated region, (19), it is noted that the first term represents the incident plane wave. The second term represents the direct reflection from the boss surface. The lines of constant phase and propagation vectors for these terms are plotted in Figure 8.

Now turning attention to the series term of (19), and applying the asymptotic form for $H_{\nu_n'}^{(1)}(k_o\rho)$ and the trigonometric identity

$$\frac{\cos \nu_n' \phi}{\sin \nu_n' \pi} e^{-i\nu_n' \pi/2} = -i \frac{e^{i\nu_n'(3\pi/2 + \phi)} + e^{i\nu_n'(3\pi/2 - \phi)}}{1 - e^{i\nu_n' 2\pi}}$$

the series becomes

$$-\frac{H_o e^{i\pi/12}}{\sqrt{2\pi k_o \sqrt{\rho^2 - a^2}}} \left(\frac{k_o a}{2}\right)^{1/3} \sum_{n=1}^{\infty}{}' D_n^{(m)} \left\{ e^{i[k_o\sqrt{\rho^2 - a^2} + \nu_n'(3\pi/2 + \phi - \arccos a/\rho)]} + e^{i[k_o\sqrt{\rho^2 - a^2} + \nu_n'(3\pi/2 - \phi - \arccos a/\rho)]} \right\}.$$

As was done for the shadow region, the lines of constant phase are plotted for $\nu_n' \sim k_o a$ in Figure 9 and Figure 10.

From the previous discussion, it is clear that four terms exist in the illuminated region. The first is the incident wave. The second is the wave reflected from the cylindrical surface. The third term is the wave which struck the cylinder at 90 degrees, traveled along the cylinder surface to 180 degrees, and was reflected back along the surface directly to the field point. The fourth term travels a path similar to the third, but radiates

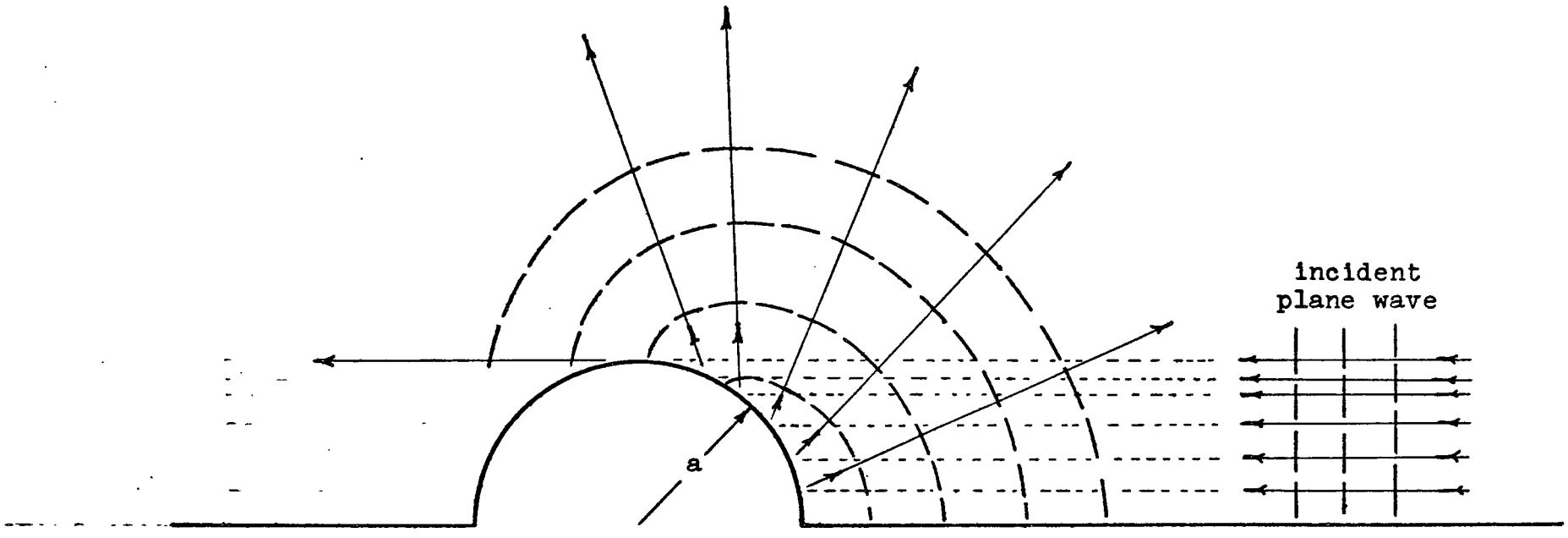

Figure 8. Lines of constant phase and propagation vectors for the terms $e^{-ik_0\rho\cos\phi}$ (incident plane wave) and $e^{ik_0(\sqrt{\rho^2-a^2\sin^2\beta}-2a\cos\beta)}$ (boss reflected wave).
— — — — — — — — lines of constant phase, ←———— propagation vectors.

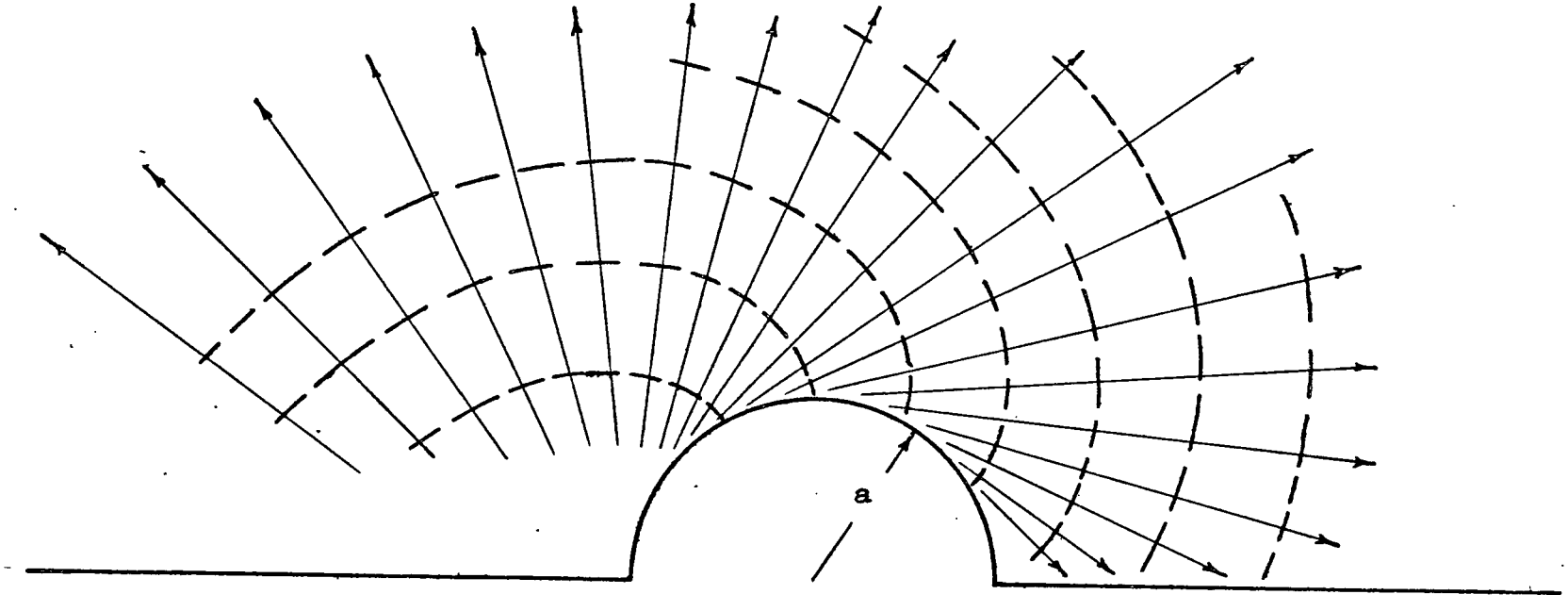

Figure 9. Lines of constant phase and propagation vectors for the term $e^{i[k_0\sqrt{\rho^2-a^2} + \nu_n'(3\pi/2 - \varphi - \arccos a/\rho)]}$, --------- lines of constant phase, ←——— propagation vectors.

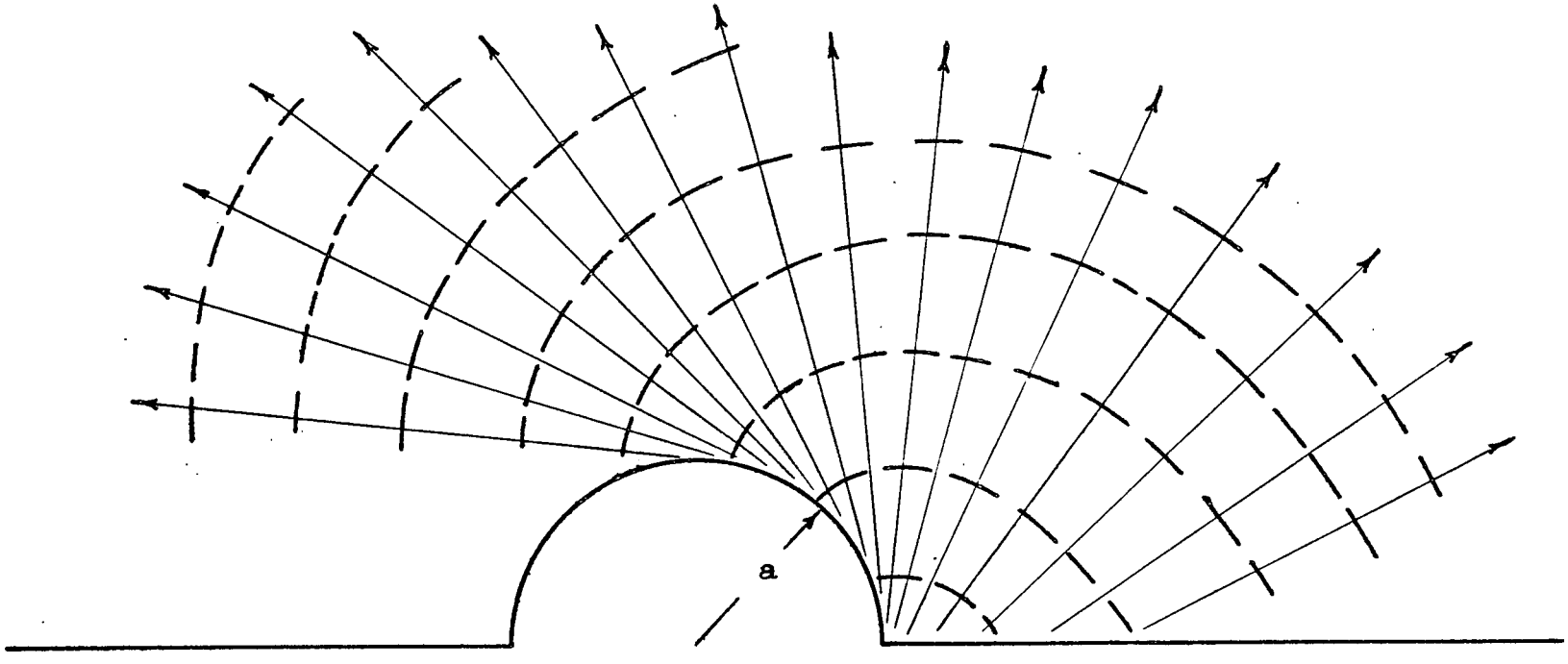

Figure 10. Lines of constant phase and propagation vectors for the term $e^{i[k_0\sqrt{\rho^2-a^2}+\nu_n'(3\pi/2+\phi-\arccos a/\rho)]}$, ---------- lines of constant phase, ←——— propagation vectors.

toward the image of the field point and is reflected by the ground plane in the illuminated region. The third and fourth terms are "creeping wave" terms.

Figures 11 (a) and (b) illustrate these four terms in ray form.

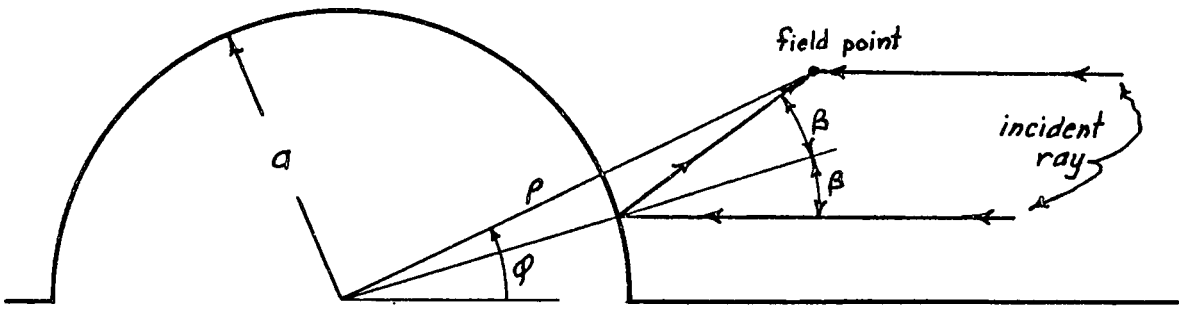

(a) Incident and reflected rays

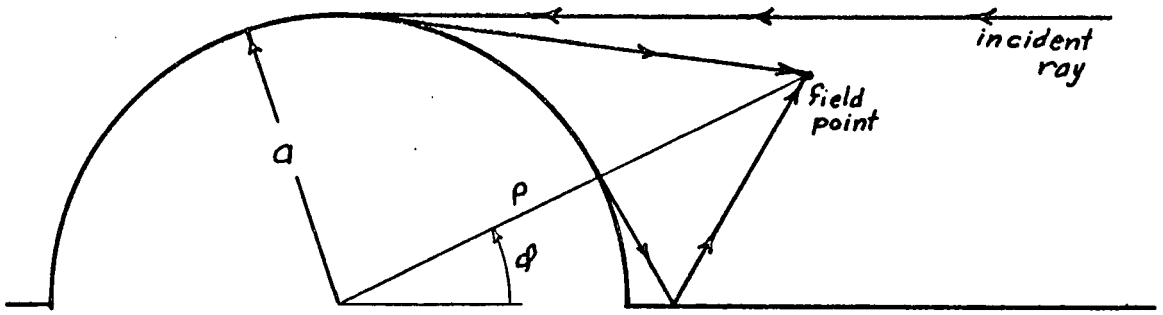

(b) Creeping wave rays

Figure 11. Illuminated region waves in ray form.

CHAPTER 3

FIELD EVALUATION FOR OBLIQUE PLANE WAVE INCIDENCE

The previous discussion involved plane ground wave diffraction. It is the simplest problem to approach and solve. The interpretation of its solutions is relatively straightforward. This, the simpler problem, has allowed familiarization with both the mathematics and the physical interpretation techniques. It has provided the foundation for approaching the problem of diffraction by a semicylindrical boss with oblique plane wave incidence.

3.1 Polarization with the Magnetic Field in the Horizontal Plane.

The problem of a vertically polarized plane wave obliquely incident on the boss is merely a generalization of the ground wave problem. In the ground wave problem the incidence angle, φ', is set at zero degrees. In the problem at hand, it remains as a variable.

Returning to (6) and allowing ρ' to approach infinity, the magnetic field intensity is found to be

$$H_z = \frac{H_o}{2}\sum_{m=0}^{\infty} \epsilon_m (-i)^m \, 2 \cos m\varphi \cos m\varphi' \cdot \left\{ J_m(k_o\rho) - \frac{J_m'(k_o a)}{H_m^{(1)\prime}(k_o a)} H_m^{(1)}(k_o\rho) \right\}, \qquad (21)$$

where $$H_o = -\frac{I^{(m)} \omega \epsilon_o}{\sqrt{2\pi k_o \rho'}} e^{i(k_o \rho' - \pi/4)}.$$

Noting the fact that the series is even and applying the relationship,

$$\cos m\phi \cos m\phi' = \frac{e^{im(\phi+\phi')} + e^{-im(\phi+\phi')} + e^{im(\phi-\phi')} + e^{-im(\phi-\phi')}}{4},$$

(21) is recast as

$$H_z = \frac{H_o}{2} \sum_{m=-\infty}^{\infty} \left[e^{im(\phi-\phi')} + e^{im(\phi+\phi')} \right] (-i)^m \left\{ J_m(k_o\rho) - \frac{J_m'(k_o a)}{H_m^{(1)\prime}(k_o a)} H_m^{(1)}(k_o\rho) \right\}. \quad (22)$$

Notice that when ϕ' is set equal to zero in (22), the solution becomes identical to the solution for ground waves given by (10).

Splitting (22) into two series,

$$H_z = S_1^{(m)} + S_2^{(m)} \quad (23)$$

where $$S_1^{(m)} = \frac{H_o}{2} \sum_{m=-\infty}^{\infty} e^{im(\phi-\phi')} (-i)^m \left\{ J_m(k_o\rho) - \frac{J_m'(k_o a)}{H_m^{(1)\prime}(k_o a)} H_m^{(1)}(k_o\rho) \right\}$$

$$S_2^{(m)} = \frac{H_o}{2} \sum_{m=-\infty}^{\infty} e^{im(\phi+\phi')} (-i)^m \left\{ J_m(k_o\rho) - \frac{J_m'(k_o a)}{H_m^{(1)\prime}(k_o a)} H_m^{(1)}(k_o\rho) \right\}$$

it is observed that $S_1^{(m)}$ and $S_2^{(m)}$ have exactly the same form as (10). Since the transformation of (10) was completed in Chapter 2, the results may be applied to each of these series.

Shadow zone. In applying the results of (10) to $S_1^{(m)}$ and $S_2^{(m)}$, it is found that the two series have different convergence requirements. That is, for $S_1^{(m)}$ the contribution of the large semicircular arc, path P_1 and P_2 in Figure 3, vanishes for field angles greater than $90 + \phi'$ degrees. For the latter series, convergence is assured only for field

angles greater than 90 - ϕ' degrees. Thus, the convergence of (23) is assured only when $\phi > \pi/2 + \phi'$. This is the shadow region on the boss, as shown in Figure 12(a).

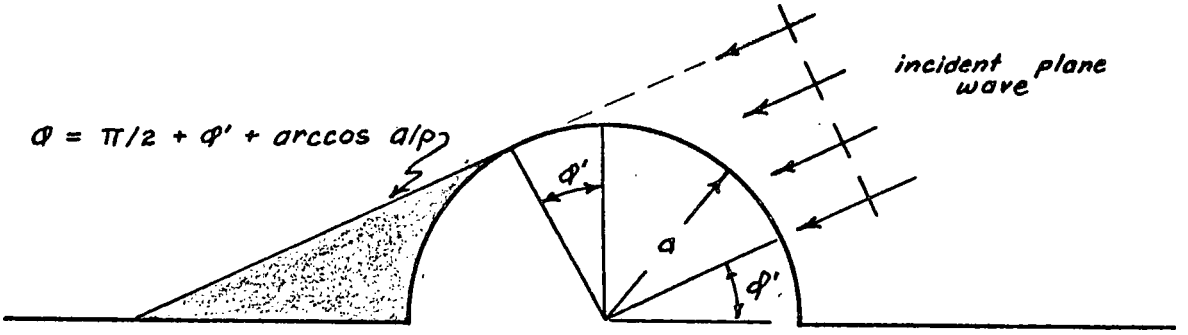

(a) Shadow region.

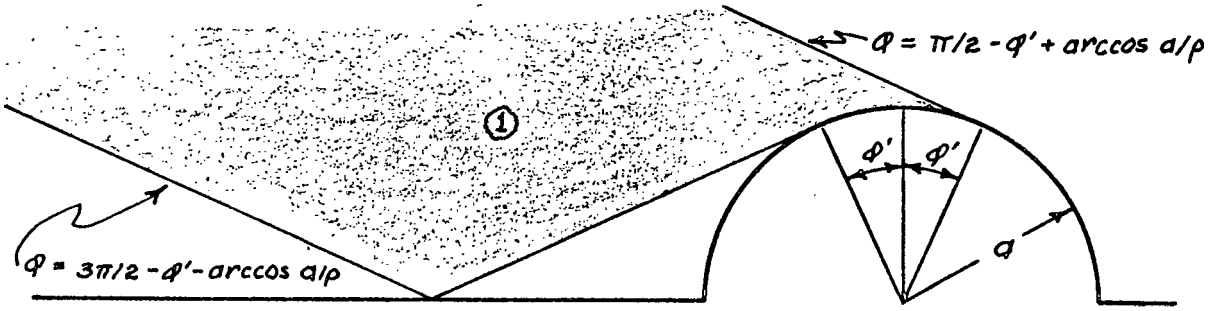

(b) Partially illuminated region.

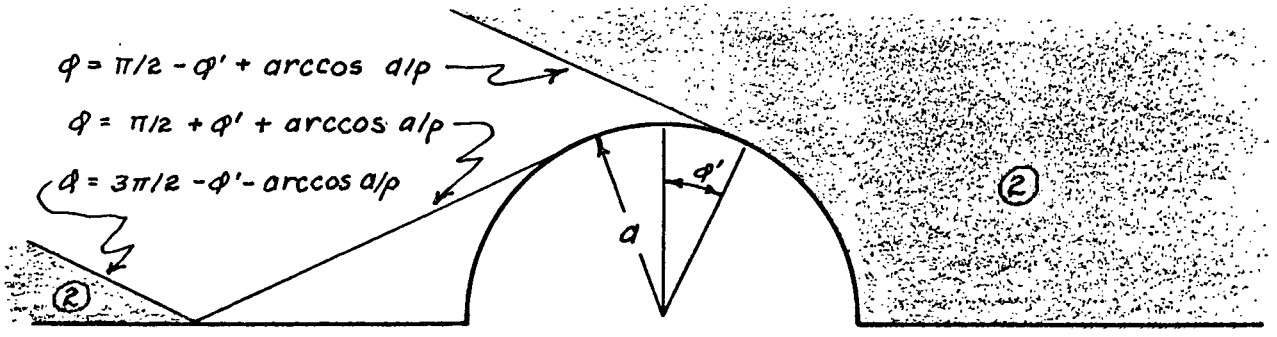

(c) Illuminated region.

Figure 12. Geometrical presentation of the regions around the semicylinderical boss.

Following the procedure for the ground wave shadow zone outlined in section 2.2, the residue series solution may be written

$$H_z = \frac{H_o}{4} e^{-i\pi/6}\left(\frac{k_o a}{2}\right)^{1/3} \sum_{n=1}^{\infty} \frac{e^{-i\nu_n'\pi/2}\, H_{\nu_n'}^{(1)}(k_o\rho)}{a_n'[Ai(a_n')]^2}\left\{\frac{\cos\nu_n'(\phi+\phi'-\pi) + \cos\nu_n'(\phi-\phi'-\pi)}{\sin\nu_n'\pi}\right\} \quad (24)$$

where ν_n' and a_n' are given in (14).

Illuminated zone. In (23), the illuminated region for $S_1^{(m)}$ includes a portion of the shadow zone of $S_2^{(m)}$, i.e. $90°-\phi'<\phi$. Thus, the illuminated region must be divided into two subregions, as shown in Figures 12(b) and (c). Region one contains the illuminated zone solution for $S_1^{(m)}$ plus the shadow zone solution for $S_2^{(m)}$. This is the partially illuminated zone. Region two contains the illuminated region solutions for both of the series in (23). This is the illuminated zone.

In keeping with the previous statements and following the procedure outlined in section 2.2, the solution in the partially illuminated zone is given as

$$\begin{aligned} H_z = \frac{H_o}{2}\Bigg\{ & \frac{1}{2} e^{-i\pi/6}\left(\frac{k_o a}{2}\right)^{1/3} \sum_{n=1}^{\infty} \frac{e^{-i\nu_n'\pi/2}\cos\nu_n'(\phi+\phi'-\pi)}{a_n'[Ai(a_n')]^2 \sin\nu_n'\pi} H_{\nu_n'}^{(1)}(k_o\rho) \\ & + \frac{1}{2} e^{-i\pi/6}\left(\frac{k_o a}{2}\right)^{1/3} \sum_{n=1}^{\infty} \frac{e^{-i\nu_n'\pi/2}\cos\nu_n'(\phi-\phi')}{a_n'[Ai(a_n')]^2 \sin\nu_n'\pi} H_{\nu_n'}^{(1)}(k_o\rho) \\ & + e^{-ik_o\rho\cos(\phi-\phi')} + \sqrt{\frac{a\cos\beta_1}{2\sqrt{\rho^2-a^2\sin^2\beta_1}-a\cos\beta_1}}\, e^{ik_o\left(\sqrt{\rho^2-a^2\sin^2\beta_1}-2a\cos\beta_1\right)}\Bigg\}, \end{aligned} \quad (25)$$

where β_1 is shown in Figure 13(a).

Now writing the solution for the illuminated zone,

$$H_z = \frac{H_o}{2}\Bigg\{ e^{-ik_o\rho\cos(\phi-\phi')} + \sqrt{\frac{a\cos\beta_1}{2\sqrt{\rho^2-a^2\sin^2\beta_1}-a\cos\beta_1}}\, e^{ik_o\left(\sqrt{\rho^2-a^2\sin^2\beta_1}-a\cos\beta_1\right)} \tag{26}$$

$$+ e^{-ik_o\rho\cos(\phi+\phi')} + \sqrt{\frac{a\cos\beta_2}{2\sqrt{\rho^2-a^2\sin^2\beta_2}-a\cos\beta_2}}\, e^{ik_o\left(\sqrt{\rho^2-a^2\sin^2\beta_2}-a\cos\beta_2\right)}$$

$$+ \frac{1}{2} e^{-i\pi/6}\left(\frac{k_o a}{2}\right)^{1/3} \sum_{n=1}^{\infty} \frac{e^{-i\nu_n'\pi/2}\, H_{\nu_n'}^{(1)}(k_o\rho)}{a_n'[Ai(a_n')]^2 \sin\nu_n'\pi}\left[\cos\nu_n'(\phi-\phi') + \cos\nu_n'(\phi+\phi')\right]\Bigg\},$$

where β_2 is shown in Figure 13(b). Note that in the limit as ρ becomes large, $\beta_1 \to (\phi-\phi')/2$ and $\beta_2 \to (\phi+\phi')/2$.

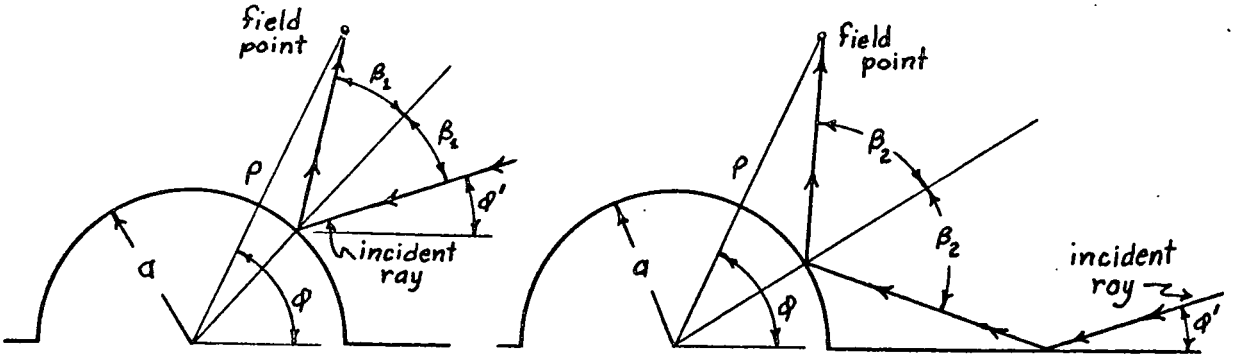

(a) (b)

Figure 13. The geometrical definition of (a) β_1 and (b) β_2 for the illuminated zone solution.

3.2 Physical Interpretation of Vertical Polarization Case.

Shadow zone. Since $S_1^{(m)}$ and $S_2^{(m)}$ are superposed to obtain the total field, the physical explanation of each series yields the total. Considering $S_1^{(m)}$ first,

$$S_1^{(m)} = \frac{H_o}{4} e^{-i\pi/6}\left(\frac{k_o a}{2}\right)^{1/3} \sum_{n=1}^{\infty} \frac{e^{-i\nu_n'\pi/2}\cos\nu_n'(\phi-\phi'-\pi)}{a_n'[Ai(a_n')]^2 \sin\nu_n'\pi}\, H_{\nu_n'}^{(1)}(k_o\rho) \tag{27}$$

Recalling that

$$\frac{e^{-i\nu_n'\pi/2}\cos\nu_n'(\phi-\phi'-\pi)}{\sin\nu_n'\pi} = -i\frac{e^{i\nu_n'(\phi-\phi'-\pi/2)} + e^{i\nu_n'(3\pi/2-\phi+\phi')}}{1-e^{i\nu_n'2\pi}}$$

and the asymptotic form of $H^{(1)}_{\nu_n'}(k_o\rho)$ for $k_o\rho > \nu_n' \sim k_o a$ (Tyras, 1969), (27) becomes

$$S_1^{(m)} = -\frac{H_o}{2}\frac{e^{i\pi/12}}{\sqrt{2\pi k_o\sqrt{\rho^2-a^2}}}\left(\frac{k_o a}{2}\right)^{1/3}\sum_{n=1}^{\infty}D_n^{(m)}\left\{e^{i[k_o\sqrt{\rho^2-a^2}+\nu_n'(\phi-\phi'-\pi/2-\arccos a/\rho)]}\right.$$
$$\left. + e^{i[k_o\sqrt{\rho^2-a^2}+\nu_n'(3\pi/2-\phi+\phi'-\arccos a/\rho)]}\right\} \qquad (28)$$

where

$$D_n^{(m)} = \frac{1}{a_n'[Ai(a_n')]^2(1-e^{i\nu_n'2\pi})}$$

It can be noted that since ν_n' has rapidly increasing positive imaginary terms, (28) is rapidly convergent for $\phi > \pi/2 + \phi' + \arccos a/\rho$. This is the shadow region as shown in Figure 12(a).

Applying the knowledge obtained from section 2.3, Figures 5 and 6, the first term in the series in (28) represents a wave which enters the boss surface at $\phi = \pi/2 + \phi'$. This wave travels at a reduced speed along the boss surface through an arc of $\phi - \pi/2 - \phi' - \arccos a/\rho$ radians, leaves the boss and arrives at the field point. This wave is shown in ray form in Figure 14(a).

The second series represents a wave which enters the boss surface at $\phi = \pi/2 - \phi'$, the image point of $\phi = 3\pi/2 + \phi'$, and travels through an arc of $3\pi/2 - \phi + \phi' - \arccos a/\rho$. This ray then leaves the boss traveling toward the image of the field point in the ground plane. It is reflected accord-

ing to Snell's law onto the field point. This ray is shown in Figure 14(b).

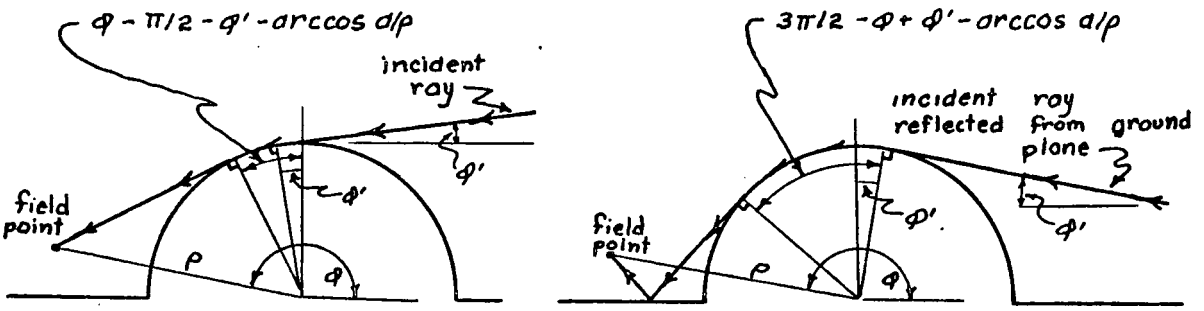

(a) (b)

Figure 14. Shadow region creeping waves and geometry in ray form for the terms, (a) $e^{i[k_0\sqrt{\rho^2-a^2}+\nu_n'(\phi-\phi'-\pi/2-\arccos a/\rho)]}$ and (b) $e^{i[k_0\sqrt{\rho^2-a^2}+\nu_n'(3\pi/2-\phi+\phi'-\arccos a/\rho)]}$.

Now considering the interpretation of $S_2^{(m)}$, one may write

$$S_2^{(m)} = -\frac{H_0}{2}\frac{e^{i\pi/12}}{\sqrt{2\pi k_0\sqrt{\rho^2-a^2}}}\left(\frac{k_0 a}{2}\right)^{1/3}\sum_{n=1}^{\infty}D_n^{(m)}\left\{e^{i[k_0\sqrt{\rho^2-a^2}+\nu_n'(\phi+\phi'-\pi/2-\arccos a/\rho)]}\right.$$
$$\left. + e^{i[k_0\sqrt{\rho^2-a^2}+\nu_n'(3\pi/2-\phi-\phi'-\arccos a/\rho)]}\right\}, \qquad (29)$$

where $D_n^{(m)}$ is given in (28).

From the discussion of $S_1^{(m)}$, the first term in (29) represents a wave which enters the boss surface at $\phi = \pi/2 - \phi'$, travels along the surface through $\phi + \phi' - \pi/2 - \arccos a/\rho$ radians, leaves the boss and propagates to the field point. This wave is shown in Figure 15(a).

The second term in (29) yields a wave which enters at $\phi = \pi/2 + \phi'$, the image of $\phi = 3\pi/2 - \phi'$. This wave travels along the surface through $3\pi/2 + \phi' - \phi - \arccos a/\rho$ radians. It then radiates toward the image of the field point, is

reflected and arrives at the field point. This ray is shown in Figure 15(b).

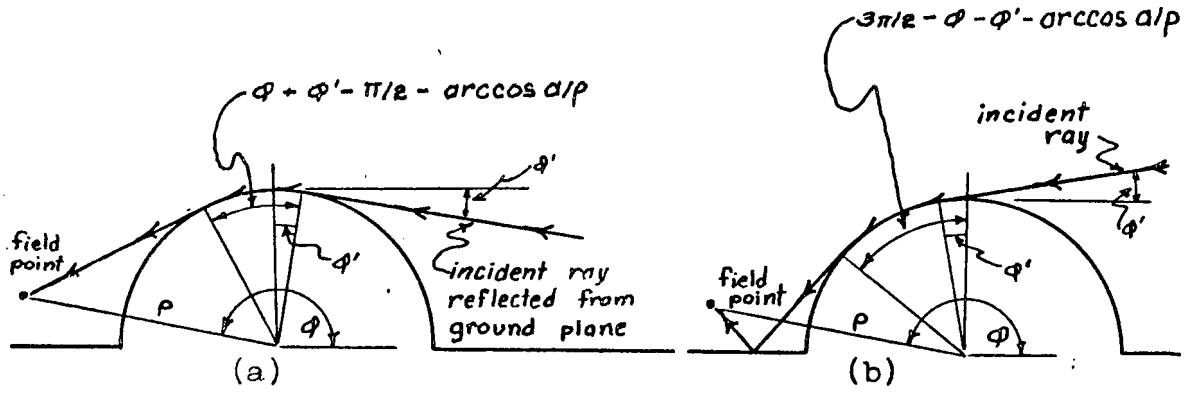

Figure 15. Shadow region creeping waves and geometry in ray form for the terms, (a) $e^{i[k_0\sqrt{\rho^2-a^2} + \nu_n'(\phi+\phi'-\pi/2-\arccos a/\rho)]}$ and (b) $e^{i[k_0\sqrt{\rho^2-a^2} + \nu_n'(3\pi/2-\phi-\phi'-\arccos a/\rho)]}$.

Notice that each series contributes one creeping wave from the incident wave and one from the wave reflected from the ground plane. This results from the fact that the original waves, because of imaging, see the boss as a complete cylinder. Series $S_1^{(m)}$ contains solutions from the original waves, while $S_2^{(m)}$ has the results of the imaging waves.

Superposition of Figure 14 and Figure 15 yields the total solution in the shadow region. This superposition is illustrated in Figure 16. Of course, the phase of the individual waves is very important in finding the numerical result.

These waves are creeping waves and have the same characteristics as those discussed in section 2.3.

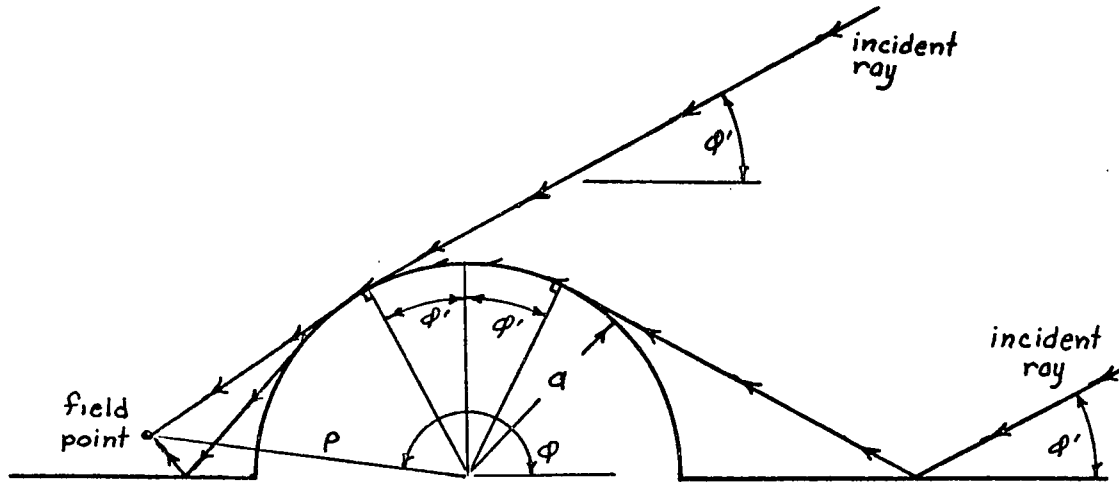

Figure 16. The graphical superposition of creeping wave terms in the shadow region. Each incident ray takes both paths in the shadow region.

Partially illuminated zone. In the partially illuminated region, the concern is with the shadow region solution of $S_2^{(m)}$ and the illuminated zone solution of $S_1^{(m)}$. Returning to (25) and performing the transformation discussed before,

$$H_z = -\frac{H_o}{2}\frac{e^{i\pi/12}}{\sqrt{2\pi k_o\sqrt{\rho^2-a^2}}}\left(\frac{k_o a}{2}\right)^{1/3}\sum_{n=1}^{\infty} D_n^{(m)} e^{ik_o\sqrt{\rho^2-a^2}}\left\{e^{i\nu_n'(\varphi+\varphi'-\pi/2-\arccos a/\rho)}\right.$$

$$+ e^{i\nu_n'(3\pi/2-\varphi-\varphi'-\arccos a/\rho)} + e^{i\nu_n'(3\pi/2+\varphi-\varphi'-\arccos a/\rho)}$$

$$\left. + e^{i\nu_n'(3\pi/2-\varphi+\varphi'-\arccos a/\rho)}\right\} + \frac{H_o}{2}\left\{e^{-ik_o\rho\cos(\varphi-\varphi')}\right.$$

$$\left. + \sqrt{\frac{a\cos\beta_1}{2\sqrt{\rho^2-a^2\sin^2\beta_1}-a\cos\beta_1}}\, e^{ik_o\left(\sqrt{\rho^2-a^2\sin^2\beta_1}-2a\cos\beta_1\right)}\right\}, \qquad (30)$$

where $D_n^{(m)}$ is given in (28) and β_1 in Figure 13(a). The first two terms of the series in (30) are illustrated in Figure 17.

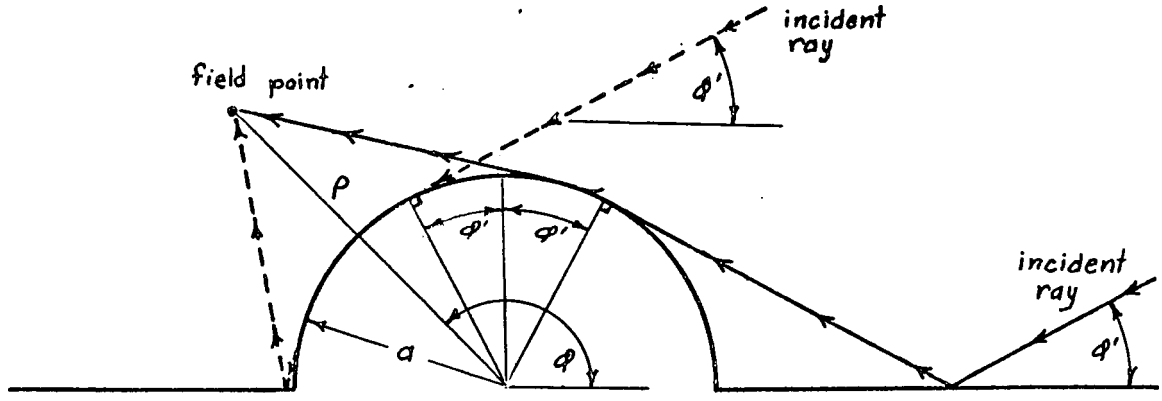

Figure 17. Partially illuminated zone creeping waves and geometry in ray form for the terms, $e^{i\nu_n'(\varphi+\varphi'-\pi/2-\arccos a/\rho)}$, ---------- $e^{i\nu_n'(3\pi/2-\varphi-\varphi'-\arccos a/\rho)}$.

The second two terms of the series are shown in Figure 18.

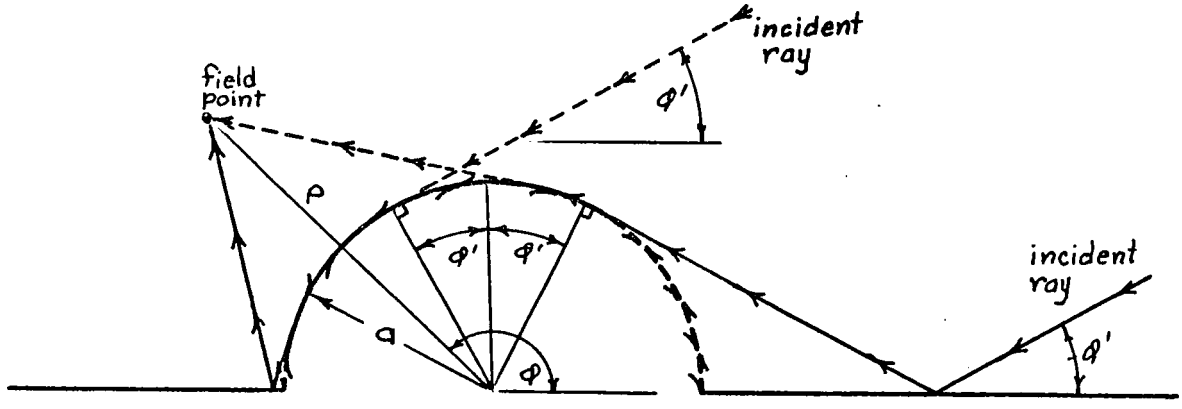

Figure 18. Partially illuminated zone creeping waves and geometry in ray form for the terms, $e^{i\nu_n'(3\pi/2-\varphi+\varphi'-\arccos a/\rho)}$, ---------- $e^{i\nu_n'(3\pi/2+\varphi-\varphi'-\arccos a/\rho)}$.

The last two terms of (30) represent the incident field and the direct reflection from the boss, as shown in Figure 19.

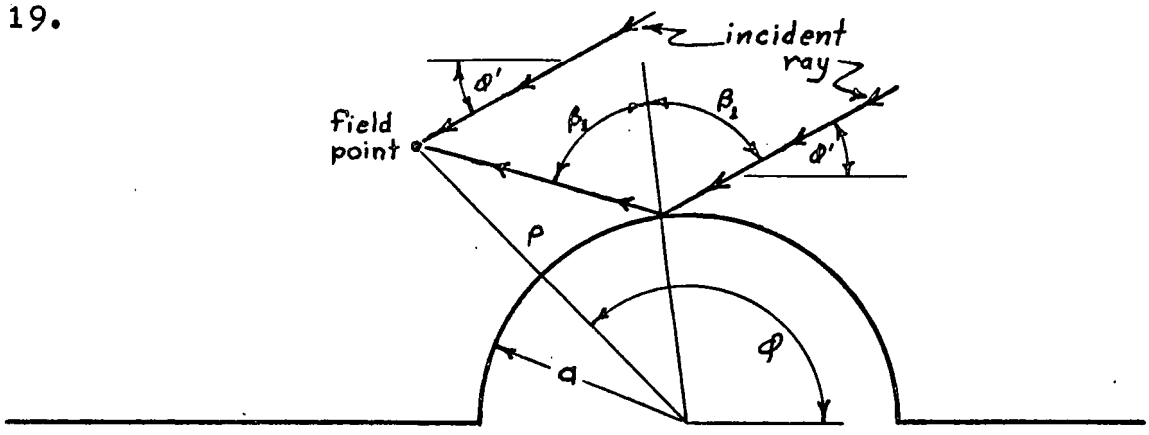

Figure 19. Partially illuminated waves in ray form that are plane incident and boss reflected.

Figures 17 and 18 show the "creeping waves".

Illuminated region. The illuminated region solution has eight terms. Four of these are "creeping waves" given by the series in (26). Two result from the incident wave as shown in Figure 20(a). The other two result from the image wave in the ground plane. These waves are shown in Figure 20(b).

The first two terms of (26) represent the direct incident wave and the direct wave reflected from the ground plane. These are shown in Figure 20(c).

The last two terms represent the reflections from the boss itself, as shown in Figure 20(d).

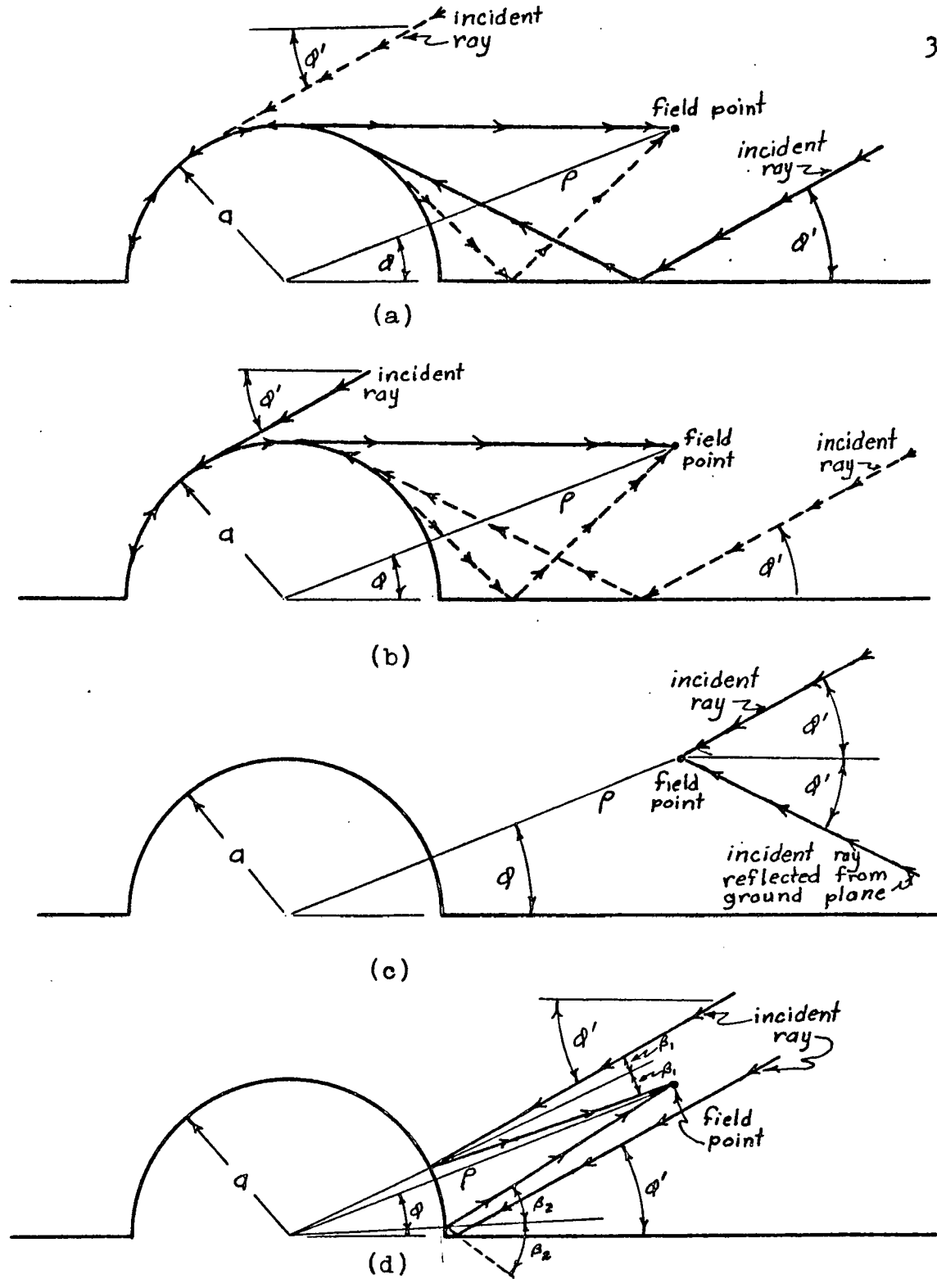

Figure 20. Illuminated zone waves in ray form, (a) creeping wave terms _____ $e^{i\nu_n'(3\pi/2-\theta+\phi'-\arccos a/\rho)}$, ----- $e^{i\nu_n'(3\pi/2+\theta-\phi'-\arccos a/\rho)}$ (b) creeping wave terms _____ $(3\pi/2-\theta-\phi'-\arccos\frac{a}{\rho})$ ---- $e^{i\nu_n'(3\pi/2+\theta+\phi'-\arccos a/\rho)}$ (c) plane wave terms one incident, one reflected from ground plane, (d) waves reflected from the boss.

It should be noted that an illuminated region exists behind the boss as shown in Figure 12(c). This is a result of $S_2^{(m)}$ having an illuminated region for $\phi > 3\pi/2 - \varphi' - \arccos a/\rho$.

A complete picture of the wave fronts of each term could be obtained by making plots like Figures 5, 6, 8, 9, and 10. This was felt to be unnecessary in this case since the ray diagrams presented give sufficient insight into the physical phenomena.

The effect of ν_n' on the solutions is the same as discussed in section 2.3. Notice that there are apparently several creeping wave modes. The first mode corresponds to ν_1', the second to ν_2', etc. The higher order modes are, however, attenuated quite rapidly. For large bosses, $k_0 a > 1$, the real part of ν_n' changes very little from mode to mode. Thus, the propagation velocity is nearly equal for each mode. On the other hand, smaller bosses, $k_0 a \rightarrow 1$, have the real part of ν_n' changing rapidly. This acts to produce large differences in phase velocity from mode to mode. It is important to note that the transformed series does not apply for $k_0 a < 1$.

3.3 Polarization with the Electric Field in the Horizontal Plane.

The problem of a horizontally polarized plane wave obliquely incident on the cylindrical boss must first be solved in the classical manner. In terms of the electric Hertzian vector, the wave equation and associated

electromagnetic fields are given by

$$(\nabla^2 + k_o^2)\,\overline{\Pi}^{(e)} = \frac{-i}{\omega \epsilon_o}\,\overline{J}^{(e)}\,, \tag{31}$$

$$\overline{E} = k_o^2\,\overline{\Pi}^{(e)} + \nabla(\nabla\cdot\overline{\Pi}^{(e)})\,, \tag{32}$$

$$\overline{H} = -i\omega\epsilon_o\,\nabla\times\overline{\Pi}^{(e)}. \tag{33}$$

The desired incident wave is obtained by expressing the electric current density, $\overline{J}^{(e)}$, as a line current located at (ρ', ϕ') by

$$\overline{J}^{(e)} = I^{(e)}\,\frac{\delta(\rho-\rho')\,\delta(\phi-\phi')}{\rho}\,\overline{a}_z$$

and then allowing ρ' to approach infinity.

As before, only the z-component of the electric Hertzian vector will exist. Thus, (31) becomes

$$\left[\frac{1}{\rho}\,\frac{\partial}{\partial\rho}\left(\rho\,\frac{\partial}{\partial\rho}\right) + \frac{1}{\rho^2}\,\frac{\partial^2}{\partial\phi^2} + k_o^2\right]\Pi_z^{(e)} = \frac{-i\,I^{(e)}}{\omega\epsilon_o}\,\frac{\delta(\rho-\rho')\,\delta(\phi-\phi')}{\rho}\,, \tag{34}$$

with boundary conditions given by

$$\Pi_z^{(e)} = 0 \qquad \text{at} \qquad \rho = a\,;\ \phi = 0, \pi\,.$$

The solution to (34) is well known and is given by, (Jones, 1964)

$$\Pi_{z\,\rho<\rho'}^{(e)} = \frac{-I^{(e)}}{\omega\epsilon_o}\sum_{m=1}^{\infty}\sin m\phi\,\sin m\phi'\,H_m^{(1)}(k_o\rho')\,\cdot \left\{J_m(k_o\rho) - \frac{J_m(k_o a)}{H_m^{(1)}(k_o a)}\,H_m^{(1)}(k_o\rho)\right\}. \tag{35}$$

The electric field intensity, (35), may be recast as

$$E_z = \frac{E_o}{2}\sum_{m=-\infty}^{\infty}\left[e^{im(\phi-\phi')} - e^{im(\phi+\phi')}\right](-i)^m \left\{J_m(k_o\rho) - \frac{J_m(k_oa)}{H_m^{(1)}(k_oa)} H_m^{(1)}(k_o\rho)\right\}. \quad (36)$$

The series given in (36) is not in a form which readily converges for $k_oa > 1$. Thus, it will be applied to the Watson Transformation.

Splitting (36) into two series,

$$E_z = S_1^{(e)} - S_2^{(e)}, \quad (37)$$

where

$$S_1^{(e)} = \frac{E_o}{2}\sum_{m=-\infty}^{\infty} e^{im(\phi-\phi')}(-i)^m \left\{J_m(k_o\rho) - \frac{J_m(k_oa)}{H_m^{(1)}(k_oa)} H_m^{(1)}(k_o\rho)\right\}$$

$$S_2^{(e)} = \frac{E_o}{2}\sum_{m=-\infty}^{\infty} e^{im(\phi+\phi')}(-i)^m \left\{J_m(k_o\rho) - \frac{J_m(k_oa)}{H_m^{(1)}(k_oa)} H_m^{(1)}(k_o\rho)\right\}.$$

Shadow zone. Since $S_1^{(e)}$ and $S_2^{(e)}$ are similar, $S_1^{(e)}$ will be transformed and the results applied to $S_2^{(e)}$. The transformation of the electric case follows the same general procedure as the magnetic case. The difference lying in the term $J_m(k_oa)/H_m^{(1)}(k_oa)$.

Writing $S_1^{(e)}$ in integral form

$$S_1^{(e)} = \frac{i}{2}\int_C \frac{e^{i\nu(\phi-\phi'-\pi)}}{\sin \nu\pi} B_\nu^{(e)}\, d\nu, \quad (38)$$

where

$$B_\nu^{(e)} = \frac{E_o}{4}\frac{e^{-i\nu\pi/2}}{H_\nu^{(1)}(k_oa)}\left\{H_\nu^{(1)}(k_oa)\, H_\nu^{(2)}(k_o\rho) - H_\nu^{(2)}(k_oa)\, H_\nu^{(1)}(k_o\rho)\right\}$$

and C is the contour shown in Figure 2. Since $B_\nu^{(e)} = B_{-\nu}^{(e)}$, (38) becomes

$$S_1^{(e)} = i \int_{-\infty+i\epsilon}^{\infty+i\epsilon} \frac{\cos \nu(\varphi - \varphi' - \pi)}{\sin \nu\pi} B_\nu^{(e)} \, d\nu \qquad (39)$$

The integral in (39) is evaluated by closing the contour in the upper half ν- plane. In closing the contour, the poles which result from the zeroes of $H_\nu^{(1)}(k_o a)$ are captured. These poles must be excluded from the contour. Thus, the contour is taken as shown in Figure 3.

Since the contribution of P_1 and P_2 vanishes as $|\nu| \to \infty$ for $\varphi > \pi/2 + \varphi'$, the theory of residues may be applied to obtain,

$$S_1^{(e)} = \frac{E_o}{2} \pi \sum_{n=1}^{\infty} \frac{H_{\nu_n}^{(2)}(k_o a)}{\frac{\partial}{\partial \nu} H_\nu^{(1)}(k_o a)\Big|_{\nu=\nu_n}} \frac{\cos \nu_n(\varphi - \varphi' - \pi) \, e^{-i\nu_n \pi/2}}{\sin \nu_n \pi} H_{\nu_n}^{(1)}(k_o \rho) \qquad (40)$$

where ν_n is the n^{th} zero of $H_\nu^{(1)}(k_o a)$ as obtained from its Airy function representation. Also, $H_{\nu_n}^{(2)}(k_o a)$ and $\frac{\partial}{\partial \nu} H_\nu^{(1)}(k_o a)\Big|_{\nu=\nu_n}$ may be expressed by their Airy function forms (Tyras,1969), so that (40) becomes

$$S_1^{(e)} = -\frac{E_o}{4} e^{-i\pi/6} \left(\frac{k_o a}{2}\right)^{1/3} \sum_{n=1}^{\infty} \frac{\cos \nu_n(\varphi - \varphi' - \pi) \, e^{-i\nu_n \pi/2}}{[Ai'(a_n)]^2 \sin \nu_n \pi} H_{\nu_n}^{(1)}(k_o \rho) \qquad (41)$$

where $$\nu_n = k_o a - a_n \left(\frac{k_o a}{2}\right)^{1/3} e^{i\pi/3}$$

and a_n are the zeroes of the Airy function. The prime of the Airy function denotes the derivative with respect to the Airy function argument.

Performing the transformation of $S_2^{(e)}$,

$$S_2^{(e)} = -\frac{E_o}{4} e^{-i\pi/6}\left(\frac{k_o a}{2}\right)^{1/3} \sum_{n=1}^{\infty} \frac{\cos \nu_n(\phi+\phi'-\pi)\, e^{-i\nu_n\pi/2}}{[Ai'(a_n)]^2 \sin \nu_n \pi} H_{\nu_n}^{(1)}(k_o\rho) \qquad (42)$$

Putting (41) and (42) back into (37),

$$E_z = -\frac{E_o}{4} e^{-i\pi/6}\left(\frac{k_o a}{2}\right)^{1/3} \sum_{n=1}^{\infty} \frac{e^{-i\nu_n\pi/2}\, H_{\nu_n}^{(1)}(k_o\rho)}{[Ai'(a_n)]^2 \sin \nu_n \pi} \cdot \left\{\cos \nu_n(\phi-\phi'-\pi) - \cos \nu_n(\phi+\phi'-\pi)\right\}. \qquad (43)$$

This is the solution for the shadow region, $\phi > \pi/2 + \phi'$, as shown in Figure 12(a).

Illuminated zone. As was done in the magnetic case, the illuminated zone is divided into two regions as shown in Figures 12(b) and (c). The solution in the partially illuminated region includes the illuminated zone solution of $S_1^{(e)}$, (37) and the shadow zone solution of $S_2^{(e)}$.

The illuminated zone solution of $S_1^{(e)}$ is evaluated and these results applied to $S_2^{(e)}$. Noting the relationship,

$$\cos \nu(\phi-\phi'-\pi) = e^{i\nu\pi} \cos \nu(\phi-\phi') - i\, e^{i\nu(\phi-\phi')} \sin \nu\pi$$

(39) may be recast as

$$S_1^{(e)} = \int_{-\infty+i\epsilon}^{\infty+i\epsilon} \left\{e^{i\nu(\phi-\phi')} + i\frac{e^{i\nu\pi} \cos \nu(\phi-\phi')}{\sin \nu\pi}\right\} B_\nu^{(e)}\, d\nu \qquad (44)$$

The second term in the integral of (44) has been evaluated previously. Thus, (44) becomes,

$$S_1^{(e)} = -\frac{E_o}{4} e^{-i\pi/6}\left(\frac{k_o a}{2}\right)^{1/3}\sum_{n=1}^{\infty}\frac{\cos\nu_n(\phi-\phi')\,e^{-i\nu_n\pi/2}}{[Ai'(a_n)]^2\sin\nu_n\pi}H_{\nu_n}^{(1)}(k_o\rho)$$

$$+\int_{-\infty+i\epsilon}^{\infty+i\epsilon} B_\nu^{(e)}\, e^{i\nu(\phi-\phi')}\,d\nu \qquad (45)$$

Substituting $B_\nu^{(e)}$ into the remaining integral, one obtains

$$\int_{-\infty+i\epsilon}^{\infty+i\epsilon} B_\nu^{(e)} e^{i\nu(\phi-\phi')}d\nu = \int_{-\infty+i\epsilon}^{\infty+i\epsilon}\frac{E_o}{4}H_\nu^{(2)}(k_o\rho)\,d\nu \qquad (46)$$

$$-\frac{E_o}{4}\int_{-\infty+i\epsilon}^{\infty+i\epsilon}\frac{H_\nu^{(2)}(k_o a)}{H_\nu^{(1)}(k_o a)}H_\nu^{(1)}(k_o\rho)\,e^{i\nu(\phi-\phi'-\pi/2)}d\nu .$$

The first integral of (46) is zero, since $H_\nu^{(2)}(k_o\rho)$ has no poles in the upper-half ν-plane. The second integral is evaluated by the method of stationary phase to be to the first order,

$$\int_{-\infty+i\epsilon}^{\infty+i\epsilon} B_\nu^{(e)} e^{i\nu(\phi-\phi')}d\nu = \frac{E_o}{2}\left\{ e^{-ik_o\rho\cos(\phi-\phi')}\right. \qquad (47)$$

$$\left. -\sqrt{\frac{a\cos\beta_1}{2\sqrt{\rho^2-a^2\sin^2\beta_1}-a\cos\beta_1}}\,e^{ik_o\left(\sqrt{\rho^2-a^2\sin^2\beta_1}-2a\cos\beta_1\right)}\right\},$$

where β_1 is shown in Figure 13(a).

Collecting all the terms,

$$S_1^{(e)} = -\frac{E_o}{4}e^{-i\pi/6}\left(\frac{k_o a}{2}\right)^{1/3}\sum_{n=1}^{\infty}\frac{\cos\nu_n(\phi-\phi')\,e^{-i\nu_n\pi/2}}{[Ai'(a_n)]^2\sin\nu_n\pi}H_{\nu_n}^{(1)}(k_o\rho) \qquad (48)$$

$$+\frac{E_o}{2}e^{-ik_o\rho\cos(\phi-\phi')}-\frac{E_o}{2}\sqrt{\frac{a\cos\beta_1}{2\sqrt{\rho^2-a^2\sin^2\beta_1}-a\cos\beta_1}}\,e^{ik_o\left(\sqrt{\rho^2-a^2\sin^2\beta_1}-2a\cos\beta_1\right)}.$$

Now applying the results of (48) and (42) to (37), the solution for the partially illuminated zone is given as,

$$E_z = \frac{E_o}{2}\Bigg\{e^{-ik_o\rho\cos(\phi-\phi')} - \sqrt{\frac{a\cos\beta_1}{2\sqrt{\rho^2-a^2\sin^2\beta_1}-a\cos\beta_1}}\, e^{ik_o\left(\sqrt{\rho^2-a^2\sin^2\beta_1}-2a\cos\beta_1\right)} - \frac{1}{2}e^{-i\pi/6}\left(\frac{k_o a}{2}\right)^{1/3}\sum_{n=1}^{\infty}\frac{e^{-i\nu_n\pi/2}\,H_{\nu_n}^{(1)}(k_o\rho)}{[Ai'(a_n)]^2\sin\nu_n\pi}\left[\cos\nu_n(\phi-\phi') - \cos\nu_n(\phi+\phi'-\pi)\right]\Bigg\}. \tag{49}$$

Next, the results of the solution for $S_1^{(e)}$ in the illuminated zone are applied to $S_2^{(e)}$ to obtain,

$$S_2^{(e)} = \frac{E_o}{2}\Bigg\{\frac{1}{2}e^{-i\pi/6}\left(\frac{k_o a}{2}\right)^{1/3}\sum_{n=1}^{\infty}\frac{\cos\nu_n(\phi+\phi')\,e^{-i\nu_n\pi/2}}{[Ai'(a_n)]^2\sin\nu_n\pi}\,H_{\nu_n}^{(1)}(k_o\rho) + e^{-ik_o\rho\cos(\phi+\phi')} - \sqrt{\frac{a\cos\beta_2}{2\sqrt{\rho^2-a^2\sin^2\beta_2}-a\cos\beta_2}}\, e^{ik_o\left(\sqrt{\rho^2-a^2\sin^2\beta_2}-2a\cos\beta_2\right)}\Bigg\}, \tag{50}$$

where β_2 is defined in Figure 13(b).

Putting (48) and (50) into (37), the illuminated zone solution is given as

$$E_z = \frac{E_o}{2}\Bigg\{e^{-ik_o\rho\cos(\phi-\phi')} - e^{-ik_o\rho\cos(\phi+\phi')} - \sqrt{\frac{a\cos\beta_1}{2\sqrt{\rho^2-a^2\sin^2\beta_1}-a\cos\beta_1}}\, e^{ik_o\left(\sqrt{\rho^2-a^2\sin^2\beta_1}-2a\cos\beta_1\right)} + \sqrt{\frac{a\cos\beta_2}{2\sqrt{\rho^2-a^2\sin^2\beta_2}-a\cos\beta_2}}\, e^{ik_o\left(\sqrt{\rho^2-a^2\sin^2\beta_2}-2a\cos\beta_2\right)} - \frac{1}{2}e^{-i\pi/6}\left(\frac{k_o a}{2}\right)^{1/3}\sum_{n=1}^{\infty}\frac{e^{-i\nu_n\pi/2}\,H_{\nu_n}^{(1)}(k_o\rho)}{[Ai'(a_n)]^2\sin\nu_n\pi}\left\{\cos\nu_n(\phi-\phi') - \cos\nu_n(\phi+\phi')\right\}\Bigg\}. \tag{51}$$

Figure 12(c) shows this region.

3.4 Physical Interpretation of Horizontal Polarization Case.

As before, the first step toward physical understanding is the transformation of $S_1^{(e)}$, (41), and $S_2^{(e)}$, (42). The interpretation of each series is then undertaken, and super-

position is applied to obtain the total field. It is important to notice in (37) that $S_2^{(e)}$ is subtracted from $S_1^{(e)}$.

Shadow zone. The transformation of $S_1^{(e)}$, (41), and $S_2^{(e)}$, (42), combined with (37), yields

$$E_z = \frac{E_o\, e^{i\pi/12}}{2\sqrt{2\pi k_o\sqrt{\rho^2-a^2}}}\left(\frac{k_o a}{2}\right)^{1/3}\sum_{n=1}^{\infty} D_n^{(e)}\, e^{ik_o\sqrt{\rho^2-a^2}}\Big\{ e^{i\nu_n(\phi-\phi'-\pi/2-\arccos a/\rho)} + e^{i\nu_n(3\pi/2-\phi+\phi'-\arccos a/\rho)} - e^{i\nu_n(\phi+\phi'-\pi/2-\arccos a/\rho)} - e^{i\nu_n(3\pi/2-\phi-\phi'-\arccos a/\rho)}\Big\}, \tag{52}$$

where $$D_n^{(e)} = \frac{1}{[Ai'(a_n)]^2(1-e^{i\nu_n 2\pi})}$$

The only differences between this solution, (52), and the magnetic case, (28) and (29), are the negative signs preceding the last two terms of (52). Recalling that a horizontally polarized wave is phase shifted by 180 degrees upon reflection from a perfectly conducting plane, the last two terms evidently represent waves which have been reflected an odd number of times. The first two terms must, then, represent waves which have been reflected an even number of times.

The ray diagrams for the first two terms of (52) are shown in Figure 14(a) and Figure 14(b), respectively. Notice that term one of (52) is a wave which is not reflected. Therefore, it has a positive sign. Term two of (52) is a wave which is reflected twice; once in front of the boss, and once behind the boss, as shown in Figure 14(b). It, too, has a positive sign.

The ray diagrams for the last two terms of (52) are shown in Figures 15(a) and (b). Notice that both of these rays are reflected once before arriving at the field point. Hence, the negative signs take care of the 180 degree phase change upon reflection.

Partially illuminated zone. In this zone, as in the magnetic case, the interest is in the shadow region solution of $S_2^{(e)}$ and the illuminated zone solution of $S_1^{(e)}$. Transforming the desired solutions, (49),

$$E_z = \frac{E_o}{2}\Big\{ e^{-ik_o\rho\cos(\phi-\phi')} - \sqrt{\frac{a\cos\beta_1}{2\sqrt{\rho^2-a^2\sin^2\beta_1}-a\cos\beta_1}}\, e^{ik_o\left(\sqrt{\rho^2-a^2\sin^2\beta_1}-2a\cos\beta_1\right)}$$
$$+ \frac{e^{i\pi/12}}{\sqrt{2\pi k_o\sqrt{\rho^2-a^2}}}\left(\frac{k_o a}{2}\right)^{1/3}\sum_{n=1}^{\infty} D_n^{(e)}\, e^{ik_o\sqrt{\rho^2-a^2}} \cdot \qquad (53)$$
$$\Big[e^{i\nu_n(3\pi/2+\phi-\phi'-\arccos a/\rho)} + e^{i\nu_n(3\pi/2-\phi+\phi'-\arccos a/\rho)}$$
$$- e^{i\nu_n(\phi+\phi'-\pi/2-\arccos a/\rho)} - e^{i\nu_n(3\pi/2-\phi-\phi'-\arccos a/\rho)}\Big]\Big\}.$$

The ray diagram for the last two terms in the series of (53) is shown in Figure 17. These two are reflected once. The first terms of the series are shown in Figure 18. These are rays reflected twice.

The first term of (53) is the incidence wave, while the second term is reflected directly off the boss surface. The reflection from the boss produces the negative sign. These terms are shown in Figure 19.

Illuminated zone. Transforming the series in (51), the solution for the illuminated region may be recast as,

$$E_z = \frac{E_o}{2}\Bigg\{ e^{-ik_o\rho\cos(\phi-\phi')} - e^{-ik_o\rho\cos(\phi+\phi')} \tag{54}$$

$$- \sqrt{\frac{a\cos\beta_1}{2\sqrt{\rho^2 - a^2\sin^2\beta_1} - a\cos\beta_1}}\, e^{ik_o\left(\sqrt{\rho^2 - a^2\sin^2\beta_1} - 2a\cos\beta_1\right)}$$

$$+ \sqrt{\frac{a\cos\beta_2}{2\sqrt{\rho^2 - a^2\sin^2\beta_2} - a\cos\beta_2}}\, e^{ik_o\left(\sqrt{\rho^2 - a^2\sin^2\beta_2} - 2a\cos\beta_2\right)}$$

$$+ \frac{e^{i\pi/12}}{\sqrt{2\pi k_o\sqrt{\rho^2 - a^2}}}\left(\frac{k_o a}{2}\right)^{1/3}\sum_{n=1}^{\infty} D_n^{(e)}\, e^{ik_o\sqrt{\rho^2 - a^2}}\Big[e^{i\nu_n(3\pi/2 + \phi - \phi' - \arccos a/\rho)}$$

$$+ e^{i\nu_n(3\pi/2 - \phi + \phi' - \arccos a/\rho)} - e^{i\nu_n(3\pi/2 + \phi + \phi' - \arccos a/\rho)} - e^{i\nu_n(3\pi/2 - \phi - \phi' - \arccos a/\rho)}\Big]\Bigg\}.$$

The first two terms of (54) are shown in Figure 20(c). The second two terms are shown in Figure 20(d). The first two terms of the series in (54) are shown in Figure 20(a). The last two terms are given in Figure 20(b). In every case the negative signs are associated with waves which are reflected an odd number of times, while the positive terms are waves that are reflected an even number of times.

CHAPTER 4

NUMERICAL FIELD EVALUATION

The equations for the fields in all regions of the cylindrical boss have been found. They are, however, of little value if reasonable numerical results cannot be obtained. It is then the purpose of this chapter to demonstrate their applicability. This is done by comparing previous numerical solutions of the "harmonic series" with those presented here. This will be done for a plane ground wave incident on a boss with $k_o a = 3$ (Wait and Murphy, 1958).

4.1 Comparison with Previous Ground Wave Data

The solution given in (14) is the solution for the shadow region of the boss. This solution contains the factor $H^{(1)}_{\nu'_n}(k_o\rho)$. Since our interest is in the fields very near the boss, two different asymptotic forms of $H^{(1)}_{\nu'_n}(k_o\rho)$ are required. On the boss, $\rho = a$, we require the form for $\nu'_n > k_o\rho$. On the ground planes, $\rho > a$, $\nu'_n < k_o\rho$ is used (Tyras, 1969).

Applying these forms to (14) and (19) and using the values of a'_n and $Ai(a'_n)$ (Abramowitz and Stegun, 1964), yields the normalized field intensities, H_z/H_o, near the boss. These values along with those of the "harmonic series" are plotted in Figure 21.

The shadow zone is behind the boss and on the boss for

$\varphi > 90^{\circ}$. In this region two terms, n = 2, of the series in (14) were used. It is immediately evident, therefore, that the transformed series is rapidly convergent. Also, the close agreement with previous data is obvious. Equally good agreement with previous data (Wait and Murphy, 1958) for $k_o a = 1$ and $k_o a = 2$ was obtained. However, as the boss becomes smaller, more series terms are required. This is a result of the fact that for the smaller bosses, the imaginary part of ν_n' does not increase as rapidly. The series is, therefore, not so rapidly convergent.

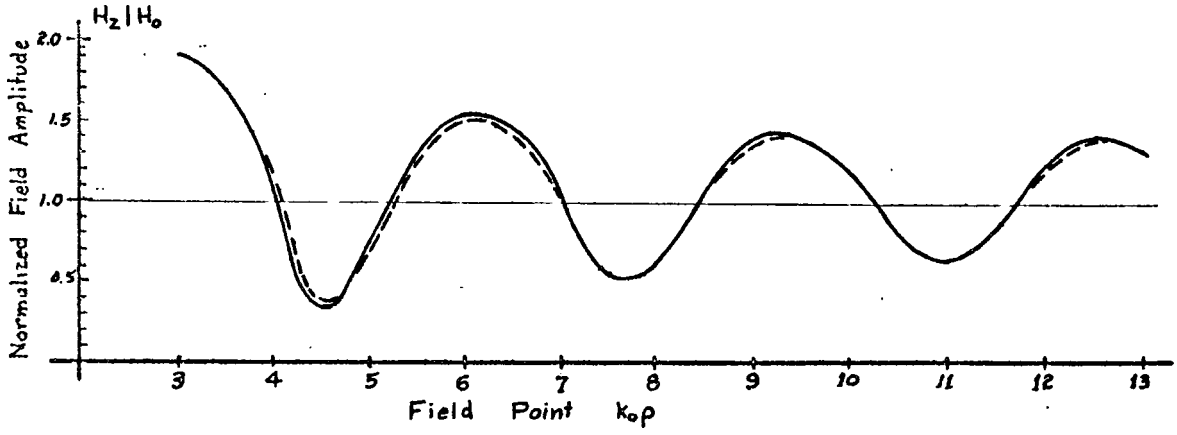

(a) Amplitude of field in front of boss ($\varphi = 0^\circ$).

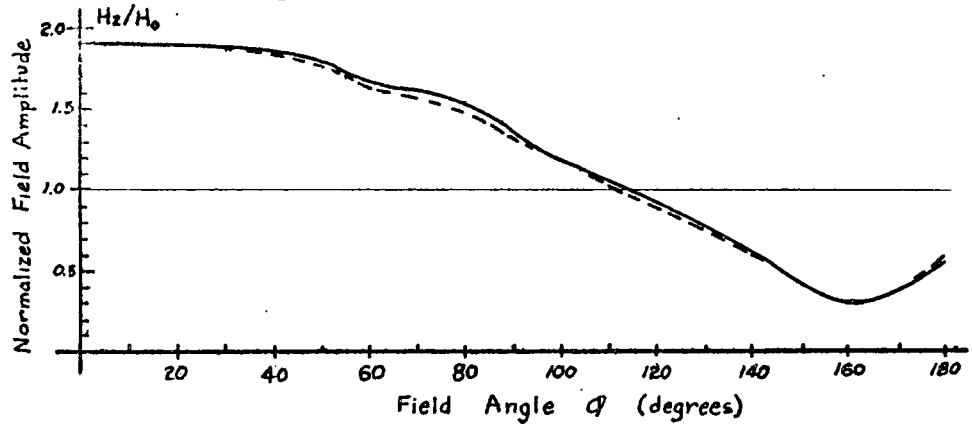

(b) Amplitude of field on boss.

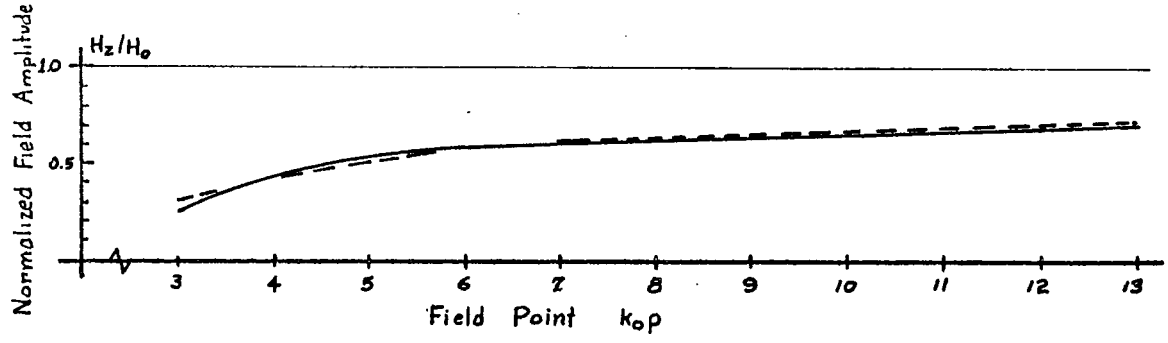

(c) Amplitude of field to rear of boss ($\varphi = 180^\circ$).

Figure 21. Normalized magnetic field amplitude in the vicinity of the boss for $k_o a = 3$. -------- Harmonic series (Wait and Murphy, 1958) ———— Transformed solution.

4.2 Comparison of Oblique Incidence with Ground Wave Incidence

The comparison of oblique plane wave incidence with plane ground wave incidence is carried out for three boss sizes, $k_o a = 5$, $k_o a = 10$, and $k_o a = 15$. Incidence angles of $\phi' = 0^\circ$ (ground wave), $\phi' = 30^\circ$ and $\phi' = 60^\circ$ are used. Figures 22, 23, and 24 show the normalized magnetic field intensity for the three bosses.

In the shadow zone, for $k_o a = 5$, two series terms are required to be within one per cent of the limit value. For $k_o a = 10$ and $k_o a = 15$, only one term is required to meet the one per cent criterion.

Upon examination, these curves give further insight into the diffraction by the boss. In the shadow region, the field increases toward its undisturbed amplitude, $H_z/H_o = 1$. This is a result of the radiation coming from the primary creeping wave which decays as it progresses around the boss. On the boss itself, the interference pattern in the shadow zone results from the phase differences between the primary creeping wave and the creeping wave reflected back along the boss. The amplitude of the reflected creeping wave becomes smaller and smaller as it progresses back toward the illuminated region. Hence, the peaks and nulls of the interference pattern become less and less pronounced.

Along the ground plane in the illuminated region, the observed pattern results from the wave reflecting off of the boss and interfering with the incident wave. Along the boss, the interference pattern is caused primarily by the incident

plane wave beating with the reflected plane wave.

In the partially illuminated region, the pattern results from the interference of the incident plane wave with the creeping wave which enters the boss at 90 - ϕ' degrees. Notice that the interference is much more pronounced near the edge of the fully illuminated zone. This is due to the diminishing amplitude of the creeping wave as it progresses through the partially illuminated zone.

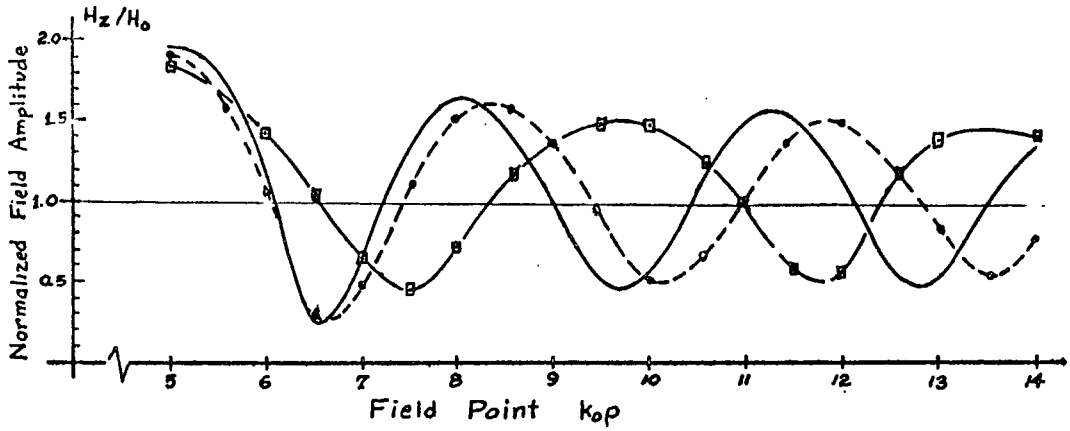

(a) Amplitude of field in front of boss ($\varphi = 0^\circ$).

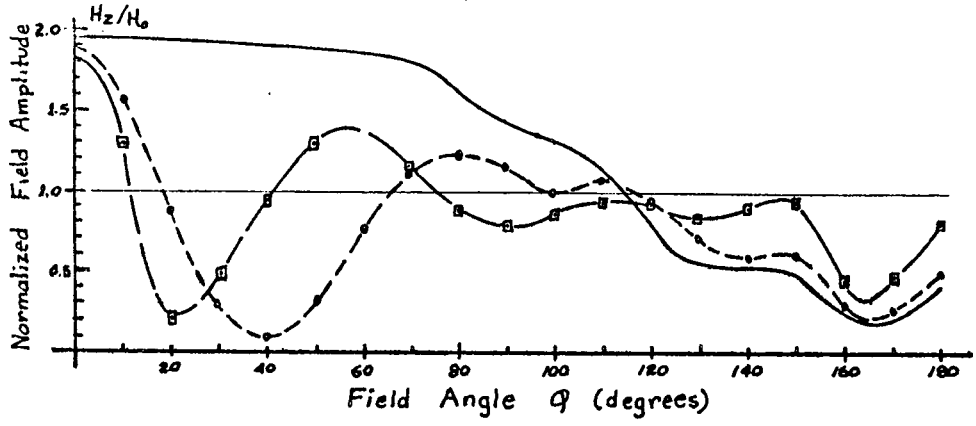

(b) Amplitude of field on boss.

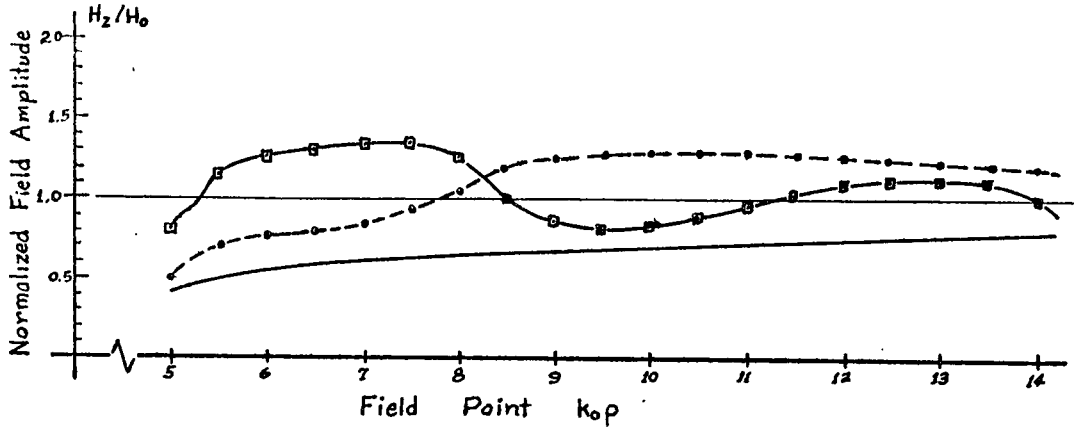

(c) Amplitude of field to rear of boss ($\varphi = 180^\circ$).

Figure 22. Normalized magnetic field amplitude in the vicinity of the boss for $k_0a = 5$. ——— $\varphi' = 0^\circ$, —·—·—·— $\varphi' = 30^\circ$, ———□———□——— $\varphi' = 60^\circ$.

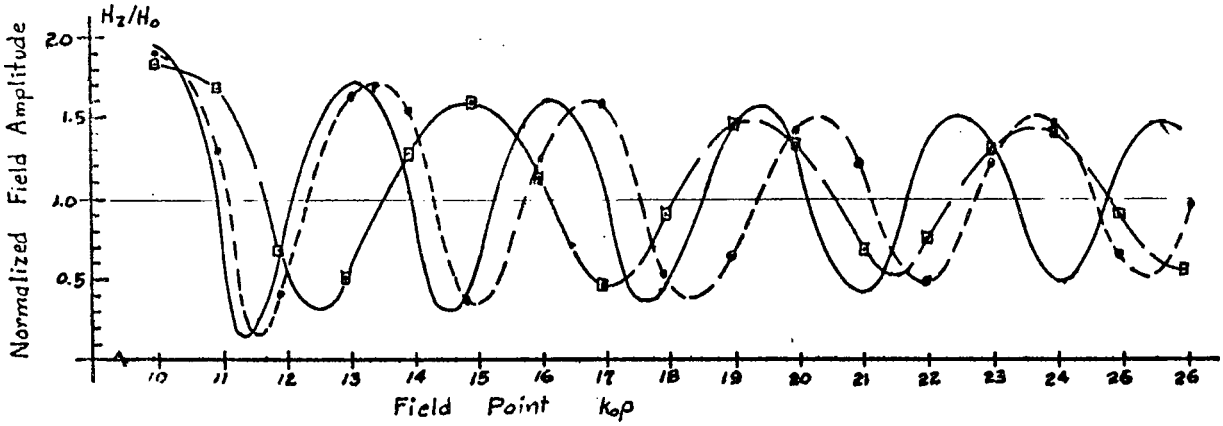

(a) Amplitude of field in front of boss ($\varphi = 0^\circ$).

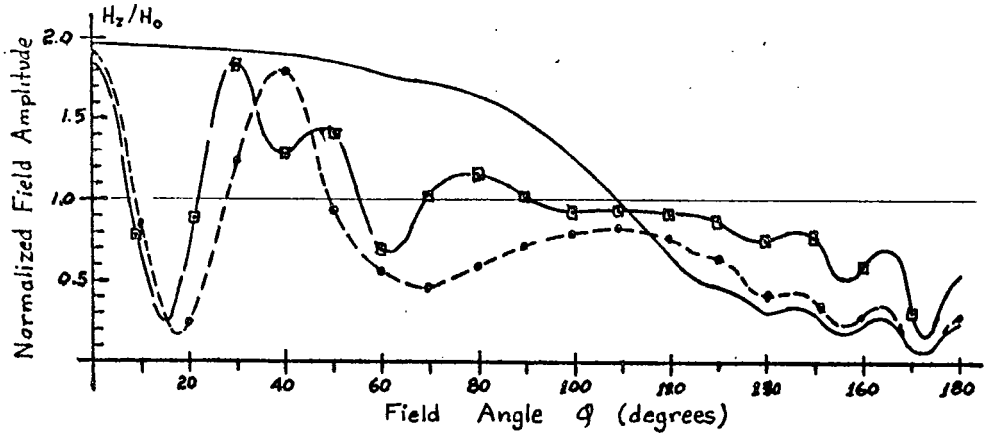

(b) Amplitude of field on boss.

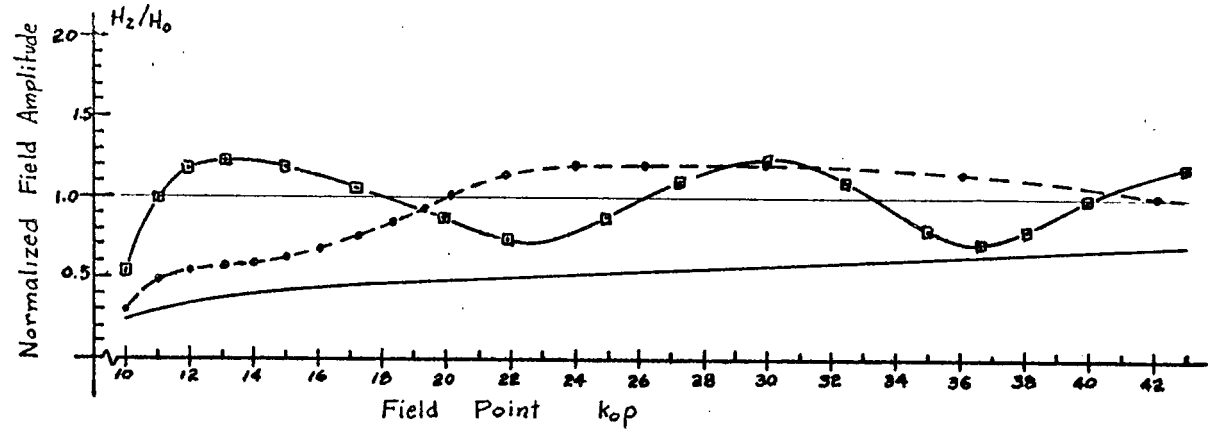

(c) Amplitude of field to rear of boss ($\varphi = 180^\circ$).

Figure 23. Normalized magnetic field amplitude in the vicinity of the boss for $k_o a = 10$. ——— $\varphi' = 0°$, – – – – $\varphi' = 30°$, ——□——□——□—— $\varphi' = 60°$.

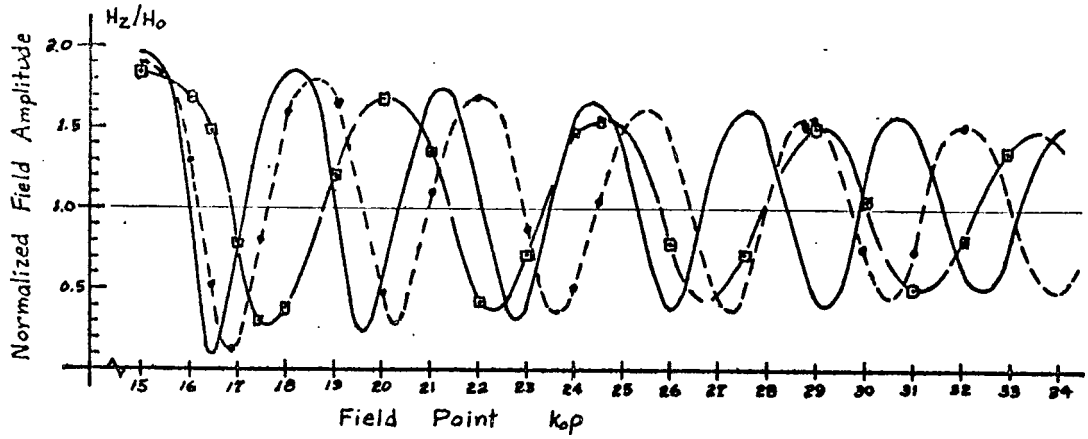

(a) Amplitude of field in front of boss ($\varphi = 0^{\circ}$).

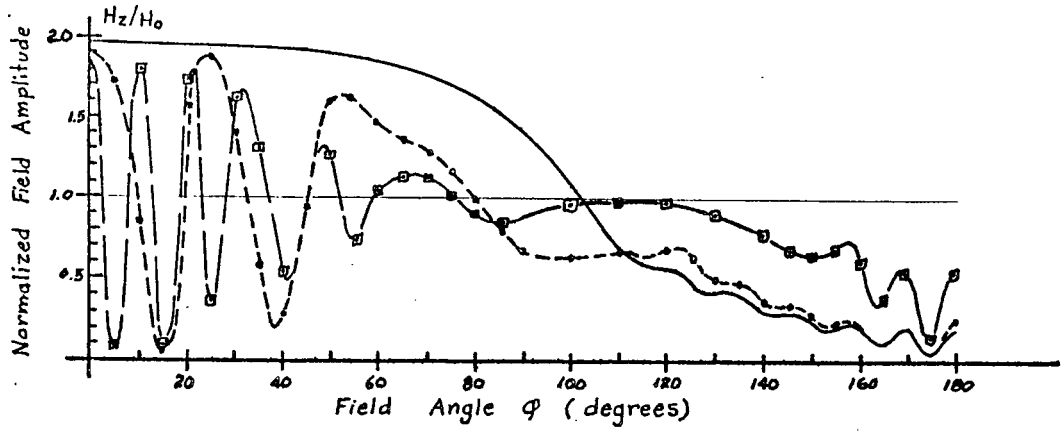

(b) Amplitude of field on boss.

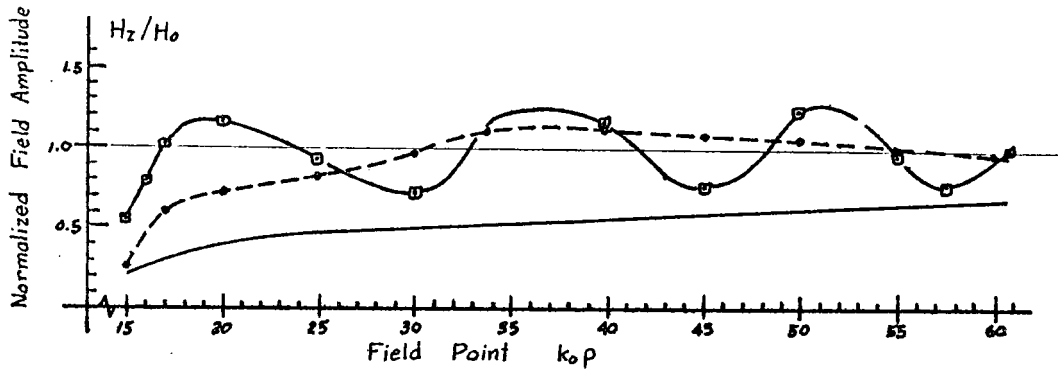

(c) Amplitude of field to rear of boss ($\varphi = 180^{\circ}$).

Figure 24. Normalized magnetic field amplitude in the vicinity of the boss for $k_o a = 15$. ——— $\varphi' = 0^{\circ}$, —·—·—·— $\varphi' = 30^{\circ}$, ——□——□——□—— $\varphi' = 60^{\circ}$.

4.3 Comparison of the Horizontal and Vertical Polarization Diffraction.

The comparison of the horizontal and vertical polarization is done for a boss of radius $k_o a = 10$, a field radius of $k_o \rho = 20$, and an incident angle of $\phi' = 30^\circ$. The interference patterns which result from the plane waves, the waves reflected from the boss, and the creeping waves are compared separately in Figure 25(a), (b) and (c), respectively. These are then superposed to obtain the total field as plotted in Figure 26. Notice that the case considered does not have a shadow zone.

As expected, Figure 25(a) and (b) show that the horizontally polarized field has nulls where the vertically polarized field has peaks. This is entirely due to the 180 degree phase shift that the horizontally polarized wave experiences upon reflection. Figure 25(c) shows that the creeping waves from the horizontal polarization are attenuated more than the vertical polarization. Also, the velocity of the horizontal creeping wave is slower. This results in a less rapid change in phase from point to point on the boss and hence, a much less pronounced interference pattern.

In superposing the results for the horizontal polarization in the partially illuminated zone, the dominant terms are the incident plane wave and the reflection off of the boss. This, however, is not true for vertical polarization. The creeping waves and the reflection from the boss are about the same amplitude.

In the illuminated region, the general character of the plane wave interference pattern is altered by the reflections from the boss. However, the location of the peaks and nulls is determined by the plane wave interference.

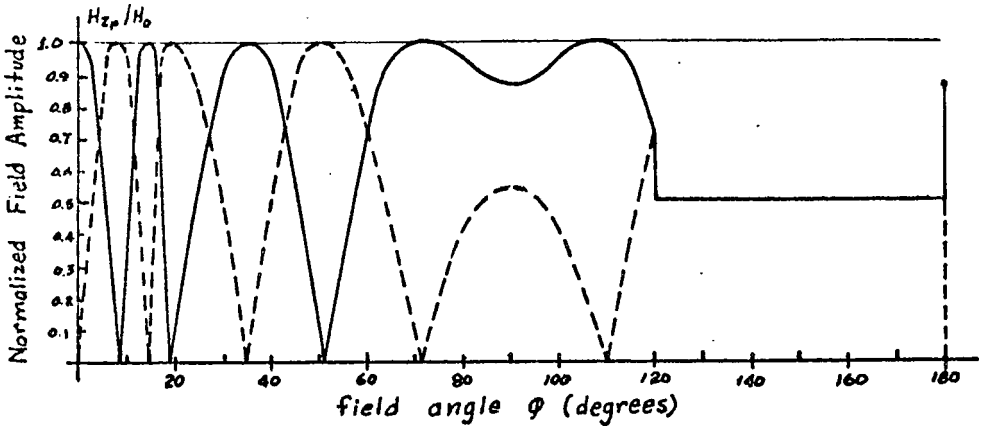

(a) Plane wave interference.

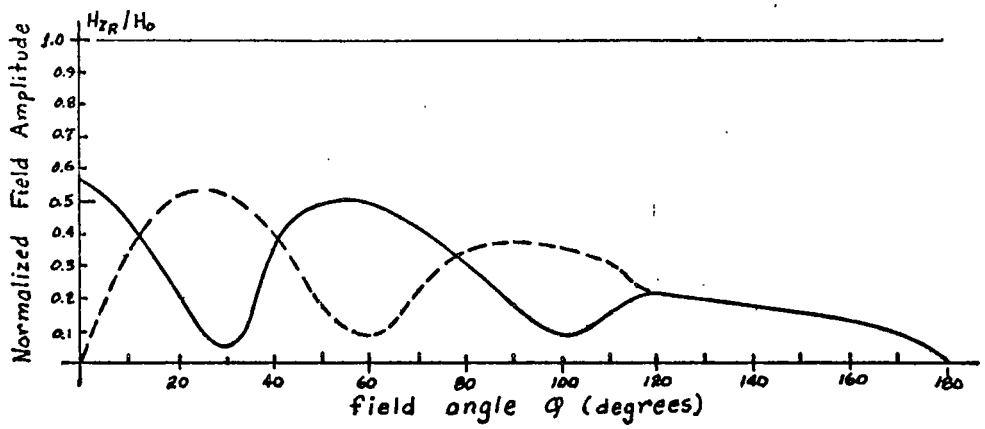

(b) Interference of waves reflected from the boss.

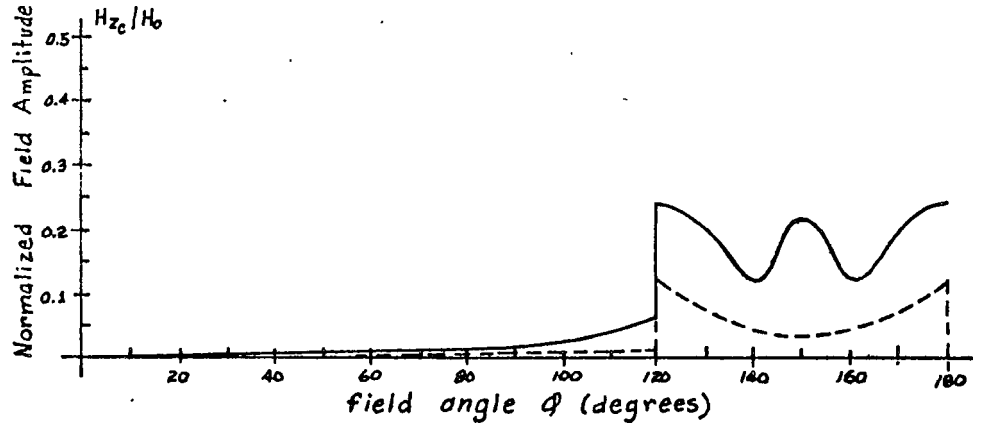

(c) Interference of creeping waves.

Figure 25. Interference patterns of terms isolated in the solution, for $k_o a = 10$, $\varphi' = 30^\circ$. -------- Horizontal polarization, ———— Vertical polarization. $K_o\rho = 20$.

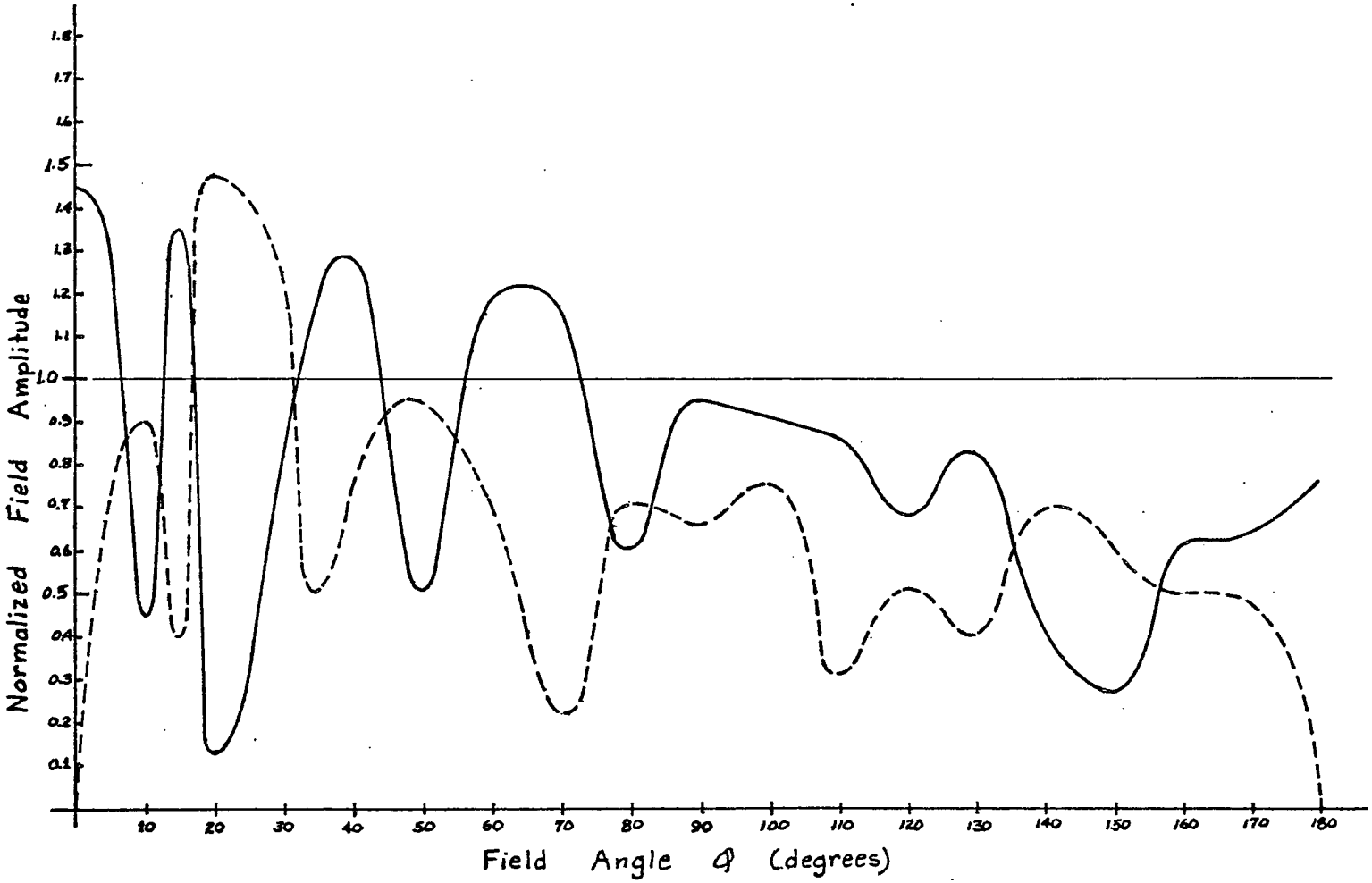

Figure 26. Normalized field amplitude at $k_0\rho = 20$ for $k_0a = 10$, $\varphi' = 30^\circ$. ---------- Horizontal polarization, ———— Vertical polarization.

4.4 Concluding Discussion

The problem solved was for perfectly conducting boundaries. Its extension to imperfectly conducting boundaries is by no means simple. However, the imperfect case can be approximated to study the influence of a ridge or island. This approximation is discussed in the following paragraphs.

It can be shown that for an imperfectly conducting boss with a high index of refraction, $n > 1$, the creeping wave terms are practically unchanged (Tyras, 1969). The earth meets this criterion. Thus, the creeping wave terms remain as given in the text.

All of the other terms in the solution result from reflections off of the boss, the flat plane, or both. In every case, the incident and reflected angles are known. By multiplying the reflection coefficient, amplitude and phase, with the appropriate terms, an approximation to the imperfect case may be obtained. Those terms which are reflected by both the flat plane and the boss require a product of reflection coefficients, one for the plane times one for the boss.

Curves of the reflection coefficient for a smooth earth and sea have been plotted for various wavelengths (Beckmann and Spizzichino, 1963). Application of this data with the solutions presented should yield a good approximation to the diffraction by a ridge or island.

A further generalization of this problem may be made by

allowing the line source to be placed at a finite distance from the origin. In this case, the term $H_\nu^{(1)}(k_o\rho')$, (6), must be included in all of the analysis. Without question, it will complicate the solution of the illuminated zone integrals and alter the form of the creeping wave terms. In addition, two solutions will result, one for $\rho>\rho'$ and one for $\rho<\rho'$.

BIBLIOGRAPHY

Abramowitz, M. and Stegun, I., Handbook of Mathematical Functions, N.B.S. Applied Mathematics Series 55, June 1964.

Beckmann, P. and Spizzichino, A., The Scattering of Electromagnetic Waves from Rough Surfaces, The Macmillan Co., 1963, pp. 220-222.

Carrier, G.F., Krook, M. and Pearson, C.E., Functions of a Complex Variable, McGraw-Hill, 1966.

Debye, P., "Mathematische Anallen", Vol. 67, 1909, pp. 535-558.

Debye, P., "Münchner Sitzungsberichte", Vol. 40, 1910.

Franz, W., Theorie der Beungung Elektromagnetischer Wellen, Springer-Verlag, 1957.

Franz, W., "Zur Asymptotik der Zylinderfunktionen undihrer Nullstellen", Z. angew. Math. Mech. Vol. 40, 1960, pp. 385.

Jones, D.S., The Theory of Electromagnetism, Macmillan Co., 1964.

Morse, P.M. and Feshbach, H., Methods of Theoretical Physics, McGraw-Hill, 1953.

Stratton, J.A., Electromagnetic Theory, McGraw-Hill, 1941, pp. 349-374, pp. 497-511.

Twersky, V., "Multiple Scattering of Radiation by an Arbitrary Planer Configuration of Parallel Cylinders and by Two Parallel Cylinders", J. Applied Physics 23, pp. 407-414, 1952.

Twersky, V., "On the Scattering of Electromagnetic Waves by Rough Surfaces", Trans. I.R.E. AP-5, pp. 81-90, 1957.

Tyras, G., Radiation and Propagation, Academic Press, 1969 (To be published).

Watson, G.N., Theory of Bessel Functions, Cambridge Univ. Press, 1962.

Wait, J.R., and Murphy, A., "Further Studies of the Influence of a Ridge on Low-Frequency Ground Wave", N.B.S. Journal of Research Vol. 61, #1, pp. 57-60, 1958.

Wait, J.R. and Murphy A., "Influence of a Ridge on the Low-Frequency Ground Wave", N.B.S. Journal of Research Vol. 58, #1, pp. 1-5, 1957.

Webster, W.P., "Field of a Magnetic Line Source in the Presence of a Semi-elliptical Boss", Master Thesis, University of Arizona, 1966.